Sl. No.	IIT Ropar List of Recent Publications with Abstract Coverage: April, 2024
A	**Book(s)**
1.	Artificial intelligence and data science based R&D interventions R Bhattacharjee, DR Neog…**SK Vipparthi** - Book, ISBN: 9789819926084, Springer, 2023 **Abstract:** Collection of massive amounts of data and the recent advances in data handling have resulted in the modern era of data-driven systems. Machine learning tools in cooperation with the data explosion and advanced computing faculties have led to a widespread development of Artificial Intelligence (AI) systems across diverse fields. As a result, data has been recognized as the new crude oil. Researchers have started to extract novel insights from the piles of data via algorithmic treatment. Within no time, strongly interdisciplinary collaborations and ventures started to evolve to adapt Data Science and Engineering to develop the desired Artificial Intelligence. The generic, mathematics-driven tools when combined with the right domain expertise have delivered sophisticated performances across a variety of deployments. Moreover, these disruptive technologies are expected to create a range of new opportunities and associated challenges in the future that cannot be foreseen yet. Based on the aforementioned, Data Science and AI are currently the most widely explored domains across diverse scientific investigations. Adapting and deploying such intelligent tools may not be straightforward in many of the use cases. The papers in this research compilation adapt different techniques from the broad areas of Data Science and Artificial Intelligence. In this book, Sarkar et al., Das et al., and Narzary et al. contribute to the broad area of Natural Language Processing (NLP). Specifically, Sarkar et al. studied the negation in Bengali language based on a corpus of Bengali words. Das et al. have investigated the neologism in Assamese language caused by the COVID-19 pandemic. They also contribute a corpus of such words in the Assamese language. Another prominent application front of AI is Computer Vision (CV). Enghi et al. proposed a deep learning-driven approach for detecting Assamese text from natural scenes. Importantly, their work develops multiple versions of deep neural network architectures for real-time detection.
2.	Process intensification for chemical and biotechnology industries SH Sonawane, **SP Gumfekar**, BA Bhanvase… - Book, ISBN: 9780323951777, Elsevier, 2024 **Abstract:** Process Intensification for Chemical Engineering and Biotechnology Industries: Fundamentals and Applications to Critical and Advanced Processes shows the importance of process intensification in the pharmaceutical, chemical, and biotechnology industries. The book provides mathematical aspects such as modeling of improved crystallization processes for the design of novel process intensification equipment. The book is an indispensable resource for researchers in the pharmaceutical, chemical, and biotechnology industries, covering the fundamentals of process intensification, equipment used for fabrication, and the implementation of novel trends in process intensification that are cost effective and produce minimum waste and high yield.
B	**Book Chapter(s)**
3.	Biomedical applications of biogenic carbon-based fluorescent nanoparticles **K Kaur, G Singh**, R Badru, N Kaur, **N Singh** - Biogenic Nanomaterial for Health and Environment: Book Chapter, 2023 **Abstract:** The wide-ranging applications of carbon dots (CDs), which can be developed using

	either green or chemical precursors, have been made possible due to their reported properties and the various precursors that have been identified. This has opened up new opportunities for the development of high-quality CDs and their use in optoelectronic devices, bioimaging, and other applications. Green precursors can be derived from fruits, vegetables, flowers, leaves, seeds, stems, crop residues, fungi/bacteria species, and waste products, while chemical precursors can be categorized as either acid reagents or non-acid reagents. It provides a brief review of the past ten years of CD synthesis using both green and chemical precursors, as well as the use of CDs as sensing materials in biomedical applications. This comprehensive review will be a valuable resource for researchers who are interested in synthesizing high-quality CDs for a variety of applications.
4.	Process intensification strategies and equipment for chemical industries SH Sonawane, ST Malkapuram…**SP Gumfekar**… - Process Intensification for Chemical and Biotechnology Industries: Book Chapter, 2024 **Abstract:** Process intensification (PI) is a new tool and it is an emerging research area in the field of chemical engineering. The PI aims to achieve sustainability by spending less capital and energy with minimal or no release of organic components into the environment and by reducing the footprint area of the plant and equipment for safety considerations. The PI technology offers plausible solution to the contemporary global challenge "to support sustainable industrial growth." There are myriad opportunities for chemical, biochemical, and allied industries, which are energy and chemical intensive, for the implementation of PI technology. Scientists firmly believe that PI technology can be used to achieve a number of Sustainable Development Goals (SDGs), particularly SDG 6, 7, 9, and 11, which are pertinent to clean water, clean energy, industry and infrastructure, and climate change, respectively.
C	**Conference Proceeding(s)**
5.	A comparative study of unsupervised learning techniques and natural language processing in network traffic classification **YP Kumar S, S Mishra,** VKC Manam - International Symposium on Advanced Networks and Telecommunication Systems (ANTS), 2023 **Abstract:** In this paper, an accurate modeling of on-chip copper interconnects with surface roughness is performed considering the parametric variability. This modeling is highly accurate as per-unit-length parameters of the on-chip rough copper interconnects are extracted via full wave EM solver. Further, a space-mapped artificial neural network (ANN) is developed for accurate prediction of eye height and eye width from the geometrical and material parameters of the rough copper interconnects. The novel space-mapping ANN developed in this work is more efficient in terms of accuracy and requires fewer training samples when compared to conventional ANNs.
6.	A low-cost dual band integratable antenna for Sub-6GHz applications Y Jiang, U Rafique, **S Agarwal**… - IEEE Microwaves, Antennas, and Propagation Conference (MAPCON), 2023 **Abstract:** In this paper, a low-cost antenna with dual band characteristics has been presented. For the first band, the proposed antenna fully covers 2.45 GHz, Wireless Local Area Network (WLAN) and Industrial, Scientific, and Medical (ISM) band covering 2.4 – 2.5 GHz band with impedance bandwidth better than -14dB. For the second band, it offers impedance bandwidth w.r.t. better than -14dB for public safety applications. Moreover, the second band also covers 4.8-5.2 GHz band w.r.t. - 10dB impedance bandwidth. It is designed using FR-4 low-cost substrate with thickness of 0.8mm. Moreover, it exhibits good radiation characteristics in terms

	of radiation patterns and gain. The shape and compactness of antenna allow its easy integration to sub-6GHz devices and IoT applications.
7.	A pulse oximeter and a controller designed for automatic regulation of oxygen concentrators **D Chowdhury, Shivdeep, DM Das** - 37th International Conference on VLSI Design and 2024 23rd International Conference on Embedded Systems (VLSID), 2024 **Abstract:** Adequate, stabilized, and continuous oxygen flow is the need of the hour for subjects with long-term respiratory ailments. This requires a huge skilled medical workforce and makes manual control very difficult, posing a threat to the lives of the subjects if they encounter under or excess oxygenation resulting in hypoxemia or hyperoxemia. This work demonstrates the design and development of a printed circuit board (PCB) prototype of a pulse oximeter that could be integrated with an oxygen concentrator to obtain an automated oxygen flow rate. Thus replacing the need for manual oxygen control and providing a more efficient and economical method for oxygenation. The designed pulse oximeter can accurately measure the blood oxygen levels and heart rate by voltage signals called Photoplethysmo-gram (PPG). The PPG signals, pulsatile due to the arterial blood flow, are derived to measure the heart rate and blood oxygen levels (SpO2). All the measured parameters are then supplied to the PC via UART. A Simulink framework is implemented to show the automated control of the oxygen flow rate through the oxygen concentrator with respect to the SpO2 measured from the pulse oximeter prototype. The design and development of this prototype propose a well-founded method to integrate the pulse oximeter with an oxygen concentrator to regulate the oxygen flow rate according to the need of the subject.
8.	Assessing the utility of GAN-Generated 3D virtual desert terrain: A user-centric evaluation of immersion and realism **RK Rai**, R Bansal, **SS Jha, R Narava** - AI Technologies and Virtual Reality: Proceedings of 7th International Conference on Artificial Intelligence and Virtual Reality (AIVR 2023), 2024 **Abstract:** Terrain modeling is increasingly becoming an essential part of robotics and virtual reality (VR). This technology has the potential to transform how robots interact with the world and how we experience virtual reality. In virtual reality, terrain models are used to create immersive and realistic landscapes for users to explore and interact with. However, creating varied, demanding, and realistic terrains in simulation is challenging and time-consuming. This paper presents an automated system capable of generating synthetic terrain and investigates how well the generated virtual terrain suits VR systems. To automate, we leverage the generative adversarial networks (GAN) with post-enhancement to generate a diverse and immersive desert. We used an actual digital elevation model (DEM) (1 m resolution) of the Mojave Desert in California, USA, obtained from the USGS agency to train the generative model. We investigated by employing a head-mounted display (HMD) for a robust quality assessment, and the results indicate our system successfully generated virtual terrain with acceptable realism.
9.	Behavioral study of the impulse waveform superimposed with sinusoidal power frequency in transmission line **M Saini, A Das, CC Reddy** - High Voltage-Energy Storage Capacitors and Their Applications: Proceedings of HV-ESCA 2023, 2024 **Abstract:** In this paper, a study of high-frequency traveling waves on a transmission line is presented. Traveling waves are voltage and current waves that travel from the source end to the load end of any power equipment, especially of a transmission line during transient conditions. Short and medium-length transmission lines are represented by equivalent T or π-model, and electrical parameters of the line are considered as lumped parameters, but this is only feasible for the steady state condition of the system. However, whenever a transient took place or in the case of a long transmission line, these parameters are treated as distributed. In a lossy transmission line, traveling waves propagate with a velocity less than the speed of light. During normal

	operating conditions, the load of the transmission line matched with the surge impedance of the transmission line to avoid any reflection. However, whenever there is a mismatch in the impedance within a transmission line or in the load, this high-frequency pulse will be reflected as well as refracted. A behavioral study of this impulse waveform can detect any possible defects or pre-fault as well as post-fault locations due to a mismatch in the total impedance of the circuit. This paper summarized the behavior study and extraction of superimposed impulse waveform with sinusoidal voltage on transmission lines for faults and defects at different locations.
10.	CoMP transmission approach for seamless connectivity in vehicular network through CRAN architecture **SK Singh,** N Gupta, **A Hari,** R Singh, **B Kumbhani** - IEEE International Conference on Advanced Networks and Telecommunications Systems (ANTS), 2023 **Abstract:** Cloud Radio Access Network (CRAN) is considered the most preferable architecture for higher frequencies (especially for mm-Wave scenarios) due to Coordinated Multi-Point (CoMP) transmission facilities. However, its potential still needs to be explored, specifically in vehicular communication. The need for extensive pre-transmission processing in a CoMP-enabled framework may become outdated for highly mobile scenarios. To address this issue, we introduce a modified integrated CRAN architecture, offering several benefits. The proposed architecture leverages both micro-wave and mm-wave technologies collaboratively to enhance the coverage of running vehicles. Furthermore, this architecture serves vehicles according to their road type, which includes: i.) Urban Areas i.e., high-traffic scenario, where the vehicles are slow-moving, and ii.) Highway, i.e., light-traffic scenario, where the vehicles are moving at high speed. Through simulation results, we demonstrate the significant performance improvements of the proposed architecture compared to traditional CRAN-based transmission.
11.	Control of five leg inverter based two motor drive under current sensor failure A Azeem, **AVR Teja, S Payami** - 2023 IEEE International Conference on Power Electronics, Smart Grid, and Renewable Energy (PESGRE), 2024 **Abstract:** This paper proposes a current sensor fault tolerant (CSFTC) control of the five-leg inverter (FLI) that drives the two induction motors independently. The simulation test validation is carried out when all current sensors or power supplies used for current sensor undergo failure. The proposed solution suggests employing generalized equations that leverage the PWM-generated voltage and the angular speed of the rotor. These equations enable the reconstruction of the stator phase current in the stationary reference frame (α-β).This scheme minimizing the system dependency on sensors in noisy environment. The proposed scheme is verified at different operating states of the drive system through the MATLAB/Simulink platform. The simulation result validate the effectiveness and feasibility of proposed scheme.
12.	Derating of a DC capacitor subjected to polarity reversal under FCG simulator application **HK Azmeera, A. P. S. Tiwana, CC Reddy, HK Gupta, P Angra** - High Voltage–Energy Storage Capacitors and Their Applications: Proceedings of HV-ESCA 2023, 2024 **Abstract:** Pulsed power applications have been a topic of extensive research in the field of defense applications with research focused on creating a non-destructible and a repeatable pulsed power system with flux compression generator (FCG) simulator topology being widely accepted. Under the influence of polarity reversals experienced in FCG simulator evident degradation of the energy storage capacitors occurs. These high voltage energy storage capacitors are nominally designed for a rated peak current and designated discharge cycles. Due to the experienced polarity reversals, the expected life of the capacitors is observed to decrease and they fail before the designated cycles. It is thus important to quantify the damage accumulated by these capacitors under polarity reversal conditions in a FCG simulator application and redesigning accordingly for this operation.
13.	Electro-magneto-hydrodynamics (EMHD) of a less conducting confined drop than the

	surrounding pool **P Gupta, P Dhar, D Samanta** - Proceedings of the 27th National and 5th International ISHMT-ASTFE Heat and Mass Transfer Conference, 2023 **Abstract:** The current work deals with the EMHD behaviour of a confined dielectric droplet suspended in another dielectric medium. It is analysed in the presence of an external electric and magnetic field. The present study is valid when the suspended droplet is less conducting than the surrounding liquid pool. The analysis adheres to the immiscible, Newtonian and leaky dielectric fluid model in the creeping flow regime under the framework of the small deformation approximation. We report that the droplet's deformation in the presence of the external electromagnetic field depends on the strength of the electromagnetic field, the mutual direction of the external magnetic field to the electric field, the thermophysical properties and the extent of confinement. The alteration in the deformation is achieved when hydrodynamic forces due to the external magnetic field either aid or oppose hydrodynamic force due to the electric field. We have also observed the phenomenon of shape reversal in the presence of an external magnetic field, which was not previously possible solely in the presence of an electric field. The presence of the external magnetic field also affects the streamline patterns within the droplet and in the surrounding pool. Thus, our results reveal that an external magnetic field can offer an alternative solution for mixing, manipulating, and transporting droplets in various microfluidic devices.
14.	Estimation of the impedance of a distributed model of a transmission line under a frequency sweep **M Kumar, A Das, CC Reddy** - High Voltage–Energy Storage Capacitors and Their Applications: Proceedings of HV-ESCA 2023, 2024 **Abstract:** In this paper, an attempt has been made to explore the driving point impedance function (DPIF) of the transmission line. This can be done by constructing the DPIF of a transmission line from sweep frequency response analysis (SFRA) data and comparing its frequency response with the measured frequency response. The DPIF has an extra edge when compared to other transfer functions since only one terminal end is required to be operated. The measured data must be represented as a polynomial in the form of "s," to construct a rational function. This rational function has to satisfy some properties so that the proposed ladder network can be synthesized. The conditions that must be satisfied are the numerically simulated data corresponds to DPIFs; the rational function generated should be real and positive. Of these, the first one can be checked by performing simulation. Carefully planned experiments are performed for this purpose. To check physical reliability, every function must conform to a Hurwitz polynomial. A generalized analytical equation for the driving point impedance function which is a function of polytopic numbers is also used for comparisons of the obtained impedance graph and derived equation. The results indicate excellent matching of frequency responses of impedance functions constructed from simulated SFRA and analytical function, thus establishing the feasibility of the application of the technique for transmission lines.
15.	Finding a promising oxide material for resistive random access memory with graphene electrode **K Varshney, M S. Yadav, DM Das, B Rawat** - 37th International Conference on VLSI Design and 2024 23rd International Conference on Embedded Systems (VLSID), 2024 **Abstract:** In this work, we attempt to find a suitable oxide resistive layer among four popular metal oxides, including HfO X , NiO X , TaO X , and TiO X for GE-based RRAM devices by investigating the device performance using a fully experimentally calibrated numerical simulation model. The results reveal that among four metal oxides, HfO X resistive layer with GE provides lower reset voltage (0.12 V), lower sneak current (81.07 nA) with better power efficiency (45.92%) for 2 8 bit capacity. On the other hand, NiO X -based RRAM shows a higher switching current (14.45 μA), more thermal stability, better uniform and distinguishable multilevel states, and higher readout margin for crossbar array size. Our study offers a

	comprehensive examination of the performance characteristics of distinct resistive layer materials that can provide an important guide to experimental efforts and trigger more efforts.
16.	Investigation of failure prevention study of coronary artery bypass grafting using computational fluid dynamics approach **AN Mallick, M Kumar, R Nadda, KM Kumar…R Repaka, A Sahani** - Proceedings of the 27th National and 5th International ISHMT-ASTFE Heat and Mass Transfer Conference, 2023 **Abstract:** A coronary artery bypass graft (CABG) enhances circulation to the heart muscle in patients with significant coronary artery disease. CABG involves grafting a healthy artery from one part of the body to the blocked coronary artery. In this work, we have performed the computational fluid dynamics (CFD) using ABAQUS finite element software to understand the effect of CABG on entirely or partially blocked coronary arteries. The effect of laminar flow was evaluated using the no-slip condition and considered the Reynolds number parameter using momentum and transport properties for the given geometric, material, and physical constraints. Based on the failure studies, we can minimize the failure of coronary arteries. Our model can help freeze optimal surgical guidelines for coronary bypass surgery such that the graft remains patent even after years of operation. The chance of failure of the heart can be minimized by the reduction in flow, velocity, and corresponding Reynolds number, accurate linear and angular positioning of the draft, and estimation of blockage size and shape. The CFD analysis of blood flow in the artery after grafting for various parameters like graft angle, blockage size, and position. At optimum graft angle, blockage position and size result in minimum velocity, and the corresponding Reynolds number lies in the artery's laminar region of blood flow.
17.	Numerical analysis of latent heat storage system for industrial process heat using phase change material for medium temperature range **K Yadav, M Agrawal, H Tyagi** - Proceedings of the 27th National and 5th International ISHMT-ASTFE Heat and Mass Transfer Conference, 2023 **Abstract:** The current need of industries is to reduce the energy consumption and move towards the utilization of renewable energy resources so that they can reduce their carbon footprints. A major part of the total energy consumption approximately 60% is used for industrial process heat with a temperature range of 60°C - 400°C. To use solar energy for such a large temperature range solar collectors such as flat plate collectors, and parabolic trough collectors are generally deployed. Further, to overcome the issue of intermittencies of solar energy latent heat energy storage systems (LHSS) provide an effective solution. LHSS overcomes these intermittencies effectively by using several phase change materials (PCM) like sugar alcohols. In the present study, a 2D numerical model has been developed and simulations have been performed on COMSOL Multiphysics for a 1 MJ storage capacity. Further, it has been tried to optimize the operating temperature variation between PCM and heat transfer fluid (HTF) using the modified heat capacity method and Boussinesq approximation for a shell-and-tube configuration. It is found that a significant difference in charging and discharging time appears due to natural convection.
18.	Postponement of dynamic Lidenfrost phenomenon during impact of oil/water (O/W) Emulsions droplet **M Meena, GVVSV Prasad, C Shekhar, P Dhar, M Sabapathy, D Samanta** - Proceedings of the 27th National and 5th International ISHMT-ASTFE Heat and Mass Transfer Conference, 2023 **Abstract:** Leidenfrost effect is the phenomenon where a droplet upon impacting on a heated surface levitates above a cushion of stable vapor layer beneath it. Leidenfrost point or temperature (LFT) is referred as the temperature at which the heat transfer performance deteriorates as the stable vapor layer acts as an insulator between the drop and the substrate.

	Delay of the Leidenfrost effect is essential to avoid burnout in several industrial applications. There have been efforts to increase the Leidenfrost point by addition of surfactants, polymers or nanobubbles to the working fluid. In addition, microtextured surfaces also proved to be useful in delaying the Leidenfrost point. The present work aims to increase the LFT by use of microemulsions of oil and water. We have shown the different impact dynamics of drops of microemulsions at various substrate temperatures. Overall, the microemulsion drops exhibited higher LFTs. The dependence of LFTs with governing parameters like Weber number and Ohnesorge number is also discussed.
19.	Preparation of three component PVDF-Bi4V2O11-SDS composites with enhanced dielectric and electrical properties RC Bag, S Moharana…**NP Mishra** … - Macromolecular Symposia, 2024 Abstract: In this work, poly(vinylidene fluoride) (PVDF)-bismuth vanadate (Bi4V2O11; BVO)-sodium dodecyl sulfate (SDS) composite films are fabricated by the solution casting method. The frequency dependence of the dielectric and electric performances of the resultant PVDF-BVO-SDS composites on various weight percentages of SDS contents is investigated. The results demonstrate that the three-component PVDF-BVO-SDS composites have a superior dielectric constant (96) and suppressed dielectric loss (<1) at 102 Hz for 20 wt% of SDS contents. The surface morphology of the PVDF-BVO-SDS composites shows that SDS is successfully reinforced on the PVDF-BVO matrix with better homogeneity. The ac conductivity of the PVDF-BVO-SDS composites is also improved, which is helpful for the enhancement of the dielectric constant and relatively low loss in the composites. Moreover, the PVDF-BVO-SDS composite also exhibits a larger value of the dielectric constant (96) than the pristine PVDF matrix, which is 15 times higher than that of the pristine one. These significantly enhanced dielectric and electrical characteristics of PVDF-BVO-SDS composites will fulfill the practical criteria for their use in high dielectric-constant capacitors and energy storage devices.
20.	Radiant air-cooling strategies for medium scale buildings using vapour absorption and cooling towers **S Kumar, G Singh, R Das** - Proceedings of the 27th National and 5th International ISHMT-ASTFE Heat and Mass Transfer Conference, 2023 **Abstract:** The motivation of the presented study is to establish a criterion for commercial building cooling systems based on radiant air-cooling (RAC) methodology. Since the RAC requires a dedicated outdoor air system (DOAS) for fresh air purpose, so two chillers are always needed. For the DOAS chiller, compression-driven arrangement is preferable, whereas, for the radiant chiller, absorption chiller may be used. For minimizing electric grid dependency, the feasibility of substituting the absorption chiller with cooling tower has been assessed for a medium scale corporate building subjected to composite meteorological conditions. Appraisal of systems' performance is gauged in terms of electrical energy consumed, coefficient of performance (CoP), room air temperature and moisture content, and the number of unfulfilled hours. EnergyPlus simulated results portray that solar energy-aided absorption system-aided RAC needs 26.17 % less primary energy than that of the cooling tower-aided RAC, because of extra load on the DOAS chiller. Despite this, thermal load delivered by the cooling tower-aided RAC is lesser, that leads the building to acquire yearly-averaged temperature of nearly 26 °C with satisfactory relative humidity below 50 %. On the other hand, solar energy-aided absorption RAC design yields an averaged relative humidity of nearly 50 %, and offers yearlyaveraged temperature of about 25 °C. As expected, CoP for absorption chiller is lower with respect to the compression chiller because of associated low grade thermal and high grade electrical energies, respectively. However, incorporation of cooling tower marginally improves the CoP of DOAS compression chiller by around 3.37 %. For cooling tower and absorption-based RAC designs, the

	number of unfulfilled hours is found to be 2.35 % and 4.92 % of the total system operational time. Encouraging scopes of research on building cooling using RAC are envisaged for the future.
21.	Residual frequency content awareness approach for image super resolution **JS Sahambi, Inderjeet** - National Conference on Communications (NCC), 2024 **Abstract:** In the past few years, several advanced techniques for enhancing the resolution of single images, known as single-image super-resolution (SISR) network methods, have emerged. Nevertheless, the majority of current approaches fail to fully exploit the information that is available before and after the convolution process, as well as the high-frequency details present in the image. In this exposition, we introduce a concise and precise super-resolution algorithm, the Residual Frequency Con-tent Awareness (RFCA) approach, with a better balance between model complexity in terms of Multi-adds (14.13G) and performance. The proposed model utilizes cascading connections to enable the learning of both low and high-frequency feature maps. The proposed RFCA method consists of Multi-Feature Aggregation (MFA), Frequency Content Awareness (FCA), and Feature Consolidation (FC) block. FCA block's purpose is to boost the high-frequency contents. The extracted feature map obtained by the MFA and FCA blocks is consolidated by the Feature Consolidation (FC) Block. This approach greatly aids in learning from high-level complex features. Visual results and quantitative metrics of PSNR and SSIM exhibit the accuracy of the proposed approach on synthetic benchmark super-resolution datasets. The experimental analysis shows that the proposed approach outperforms other existing methods for SISR in terms of memory footprint and visual quality.
22.	Seismic response of rc-framed structures on shallow rocking foundation **RM Kannan, N James, P Haldar** - International Conference on Vibration Problems, 2023 **Abstract:** Structural fuse mechanisms such as the strong column-weak beam concept, fasteners, and base isolation are typically integrated into structural elements to dissipate seismic energy exerted during earthquakes. Under-designed footing, also known as rocking footing, has been identified as one of the most effective design alternatives for isolating the superstructure from the supporting soil medium. The objective of the present study is to analyze midrise reinforced concrete frame structures on slight and heavy rocking footings and compare their responses to those of conventionally designed footings. From the nonlinear time history analysis, it has been determined that the induced moment owing to seismic action decreases by 20% for the slight rocking footing and by 50% for the severe rocking footing. In addition, there was a maximum increase in footing settlement on the order of 25–80% for footing designs with slight and heavy rocking footing, respectively. However, the settlement did not exceed permissible limits as mentioned in Indian standards. Significant rocking roof displacement is observed for dense and extremely dense soil conditions, which lowers flexural deformation in structural members. Consequently, the provision of a rocking footing demonstrates positive responses by reducing the structural demand and raising the demands on the supporting soil medium.
23.	Space mapped neuromodeling for fast & accurate signal integrity analysis of rough on-chip copper interconnects **S Kushwaha…S Pathania**, S Kumar…**R Sharma** - 2023 IEEE Electrical Design of Advanced Packaging and Systems (EDAPS), 2023 **Abstract:** In this paper, an accurate modeling of on-chip copper interconnects with surface roughness is performed considering the parametric variability. This modeling is highly accurate as per-unit-length parameters of the on-chip rough copper interconnects are extracted via full wave EM solver. Further, a space-mapped artificial neural network (ANN) is developed for accurate prediction of eye height and eye width from the geometrical and material parameters of the rough copper interconnects. The novel space-mapping ANN developed in this work is more efficient in terms of accuracy and requires fewer training samples when compared to

	conventional ANNs.
24.	Thermal analysis of effect of thermal emissivity enhancement on cooling of photovoltaic solar cell: A numerical study S Kumar, **M Agrawal, H Tyagi** - Proceedings of the 27th National and 5th International ISHMT-ASTFE Heat and Mass Transfer Conference, 2023 **Abstract:** In photovoltaic solar cells (PVC), a significant amount of irradiated solar energy is transformed into waste heat due to parasitic absorption of sub-bandgap photons. This waste heat increases the photovoltaic solar cell operating temperature which has an unfavourable impact on both its efficiency as well as its lifespan. Therefore, various active cooling techniques have been developed for thermal management of photovoltaic solar cells, but these techniques often consume significant power and can't be readily implemented. In recent days, radiative cooling of photovoltaic solar cell has attracted attention. In this paper, the impact of enhancement of thermal emissivity of top and bottom layer of photovoltaic solar cell on the maximum operating temperature of photovoltaic solar cell has been analysed by performing thermal analysis using numerical techniques. The thermal simulation results shows that enhancement of thermal emissivity has a significant impact in the reduction of maximum operating temperature which in-turn results in increased efficiency and lifespan. The simulation results show that with the thermal emissivity value of 0, the maximum operating temperature in photovoltaic solar cell is obtained to be 72.1°C and with the thermal emissivity value equal to 1, the maximum operating temperature in photovoltaic solar cell is found to be 55.1°C. Hence, there is a decrease of 17°C in maximum operating temperature of the PVC. Similarly, with enhancement in thermal emissivity from 0-0.25, 0.25-0.5, 0.5-0.75 and 0.75-1, the maximum temperature reduction is observed to be 3.9°C, 4°C, 4°C and 5.1°C respectively.
25.	Understanding the thermodynamic and kinetic behavior of the dehydrogenation process of liquid organic hydrogen carrier (Methylcyclohexane-Toluene) at high pressure **A Singh, DK Mahajan, H Tyagi** - Proceedings of the 27th National and 5th International ISHMT-ASTFE Heat and Mass Transfer Conference, 2023 **Abstract:** Fossil fuels are limited in nature and cause pollution when burn for electricity production and vehicle power generation. This necessitates an alternative renewable energy source to achieve a net-zero emission system. Hydrogen stands out as a potential energy source with a high gravimetric energy density of approximately 120 MJ/kg. However, the storage of hydrogen presents a major challenge, hindering its use as an alternative energy source for vehicles. Even though it can be stored as compressed gas or liquid, but this requires specific pressure and temperature conditions. Maintaining these conditions in turn necessitate energy-intensive heaters, chillers, and pumps. For instance, storing hydrogen as a liquid at -252°C and atmospheric pressure consumes 30% of its lower heating value. A promising technology called Liquid Organic Hydrogen Carrier (LOHC) has emerged as a solution to store hydrogen at atmospheric pressure. LOHC allows repeated hydrogenation and dehydrogenation, with the former being an exothermic process and the latter being endothermic. This technology provides a safe and efficient means of transporting and storing hydrogen for a long time and it is non-toxic and non-flammable. Due to its superior safety for hydrogen storage, LOHC should be considered as an alternative to the current fossil fuels used in light vehicles, which can leverage the existing infrastructure of petrol and diesel. This paper focuses on understanding the thermodynamic and kinetic behavior of the dehydrogenation process of LOHC (Methylcyclohexane to toluene) at high pressure by varying its pressure and temperature under limits. It is found that 90.9% dehydrogenation takes place at 300°C with 10 bar pressure which is not even possible at 450°C with 1 atm pressure at the same molar flow rate. This reduces the power required to heat the feed by almost 34%.
26.	Utilisation of wavelet entropy on EEG as an assistive tool to detect ischemic damage in brain **S Bharadwaj** - IEEE Students' Conference on Electrical, Electronics and Computer Science

	(SCEECS), 2024 **Abstract:** Focal cerebral ischemia, a neurological condition characterized by restricted blood supply to a specific area of the brain, presents a significant challenge in terms of diagnosis and treatment. Wavelet entropies are applied to assess ischemic damage in the frontoparietal, occipital, and temporal lobes of male Foster rats subjected to induced ischemia and treated with the piroxicam drug. Experimental findings highlight the high sensitivity of Shannon entropy in detecting ischemic damage in the brain, particularly at the eighth scale. Shannon and Rényi entropies exhibit high sensitivity in identifying ischemic damage across theta and alpha EEG bands in the three lobes, as well as in the frontoparietal and occipital lobes across the beta EEG band during both ischemic and recovery stages. However, Shannon entropy fails to identify ischemic damage in the frontoparietal and temporal lobes across the delta EEG band. Shannon and Rényi entropies have the potential to serve as supplementary tools for physicians in identifying ischemic damage in the brain, providing valuable insights that could enhance diagnostic and treatment strategies for ischemic patients.
D	**Journal Article(s)**
27.	A new paradigm for IRS-NOMA transmission **S Kumar,** R Singh, **B Kumbhani, S Agarwal** - IEEE Transactions on Vehicular Technology, 2024 **Abstract:** In this paper, we have analyzed the performance of a new design of the intelligent reflecting surface-non orthogonal multiple access (IRS-NOMA) system by considering all the elements of IRS to provide coherent phase shift to both users in a NOMA pair. In addition, we have designed a phase shift matrix of IRS that combines the components from IRS elements with coherent phases across both the users. The closed-form expression for the user's outage probability (OP) is derived using the Gauss-Chebyshev quadrature (GCQ) and moment-matching method to assess the system performance. Also, system throughput is evaluated in a delay-limited transmission mode. Numerical results reveal that our proposed system model of IRS-NOMA achieves better OP and higher system throughput than the other existing scenarios of IRS-NOMA networks. Finally, the Monte-Carlo simulations are also presented to verify the closed-form expressions.
28.	A novel switching vector sequencing method to optimize DC voltage ripple in dual inverter drive without affecting load current ripple **AI Gedam, KR Sekhar** - IEEE Transactions on Industrial Electronics, 2024 **Abstract:** In voltage source inverters (VSIs), the pulsewidth modulation (PWM) techniques of the inverter generate the load current ripple and dc voltage ripple. This work thoroughly analyzes the switching state correlation to optimize the dc voltage ripple without affecting the ac current ripple. The analysis revealed that the switching algorithms must act to place the switching states by computing instantaneous dc capacitor current polarity. Using the polarity information, this work proposes the novel PWM dynamic sequencing mechanism that independently places the null and active vector in the sampling time interval to accomplish the optimum dc voltage ripple. Unlike conventional PWM methodologies, a prior capacitor current polarity computation makes the proposed algorithm dynamic in realizing the optimum switching sequence at any load condition without influencing the load current ripple. Further, the proposed method identifies the dwell times from the instantaneous phase reference voltages, freeing the algorithm from complex dwell time computations and sector identification. Therefore, the proposed methodology is simple in realizing variations in PWMs by simply shifting/segregating the null time. Further, it is demonstrated that discontinuous PWMs with low current ripple can yield the lowest voltage ripple with the proposed sequence; otherwise, it is the highest among all other PWM variants.
29.	A survey on the mechanical properties of bone

	SS Barekar, SS Sarawade, **N Kumar** - Multimedia Tools and Applications, 2024 **Abstract:** The cellular component and an extracellular matrix make up the bone. Osteoblasts, bone- lining cells, osteocytes, and osteomacs that are dormant osteoblasts trapped in the extracellular matrix, make up the cellular component. An organic and a mineral phase combine to produce the matrix, which is responsible for the mechanical strength of the bone tissue. There is also a liquid component. As a result, bone has been identified as a natural composite material. “Bone is composed of roughly 60% mineral, 10% water, and 30% collagenous matrix by weight”. An increasing number of skeletal fractures are a major problem for aging populations. Given that cortical bone bears a significant portion of the physiological loading in the lower limbs, it would be ideal to comprehend the scale effects and structure–mechanical property correlations in this tissue. The quality of all these elements and their interactions play a crucial role in shaping bone's mechanical behavior. This work presents a review on 55 research works collected from the year 2008 to 2021. The basic mechanical features and behaviour of bone are discussed in this study. The "cortical bone, trabecular bone, and whole bones" are also discussed in this work along with numerous elements of material behaviour, such as flexibility, yields, fractures, tiredness, and damage. In addition, the roles of bone quantity (e.g., density, porosity) in each of the works have been analyzed. The analysis of best performance of the porosity value of the model is 44.22%, 30.34%, and 3.23% higher as compared to the other existing methods. Moreover, the research gaps and challenges of this work are addressed to enlighten future researchers.
30.	Adipose tissue macrophage-derived microRNA-210-3p disrupts systemic insulin sensitivity by silencing GLUT4 in obesity **D Patra, P Ramprasad**…**D Pal** - Journal of Biological Chemistry, 2024 **Abstract:** Management of chronic obesity-associated metabolic disorders is a key challenge for biomedical researchers. During chronic obesity, visceral adipose tissue (VAT) undergoes substantial transformation characterized by a unique lipid-rich hypoxic AT microenvironment (ATenv) which plays a crucial role in VAT dysfunction, leading to insulin resistance (IR) and type 2 diabetes(T2D). Here, we demonstrate that obese ATenv triggers the release of *miR-210-3p microRNA*-loaded extracellular vesicles (EVs) from adipose tissue macrophages (ATMs), which disseminate *miR-210-3p* to neighboring adipocytes, skeletal muscle cells, and hepatocytes through paracrine and endocrine actions, thereby influencing insulin sensitivity. Moreover, EVs collected from Dicer-silenced *miR-210-3p*-overexpressed bone marrow-derived macrophages (BMDMs), induce glucose intolerance and IR in lean mice. Mechanistically, *miR-210-3p* interacts with the 3′-UTR of GLUT4 mRNA and silences its expression, compromising cellular glucose uptake and insulin sensitivity. Therapeutic inhibition of *miR-210-3p* in VAT notably rescues high-fat diet (HFD)-fed mice from obesity-induced systemic glucose intolerance. Thus, targeting ATM-specific *miR-210-3p* during obesity could be a promising strategy for managing IR and T2D.
31.	Allylsilane as a versatile handle in photoredox catalysis **N Lal, SB Shirsath, P Singh, Deepshikha, AC Shaikh** - Chemical Communications, 2024 **Abstract:** Organosilanes have secured a special place in the synthetic world for several decades. However, among them, allylsilanes are a choice reagent for organic chemists to develop novel organic transformations. In recent years researchers have proved that visible-light photoredox catalysis has emerged as one of the most mild, sustainable, straightforward, and efficient strategies to construct simple to complex molecules with or without enantioselectivity. This review provides an in-depth analysis of recent advances and strategies employed in visible-light photoredox catalysis for allylsilane and its analogues for the development of various organic transformations. The review is divided into sections, each focused on a specific reactivity of

	allylsilane under light irradiation with C(sp2) center arene or alkene, C(sp2) center carbonyl, and C(sp3) center carbon functionality. In this review, we present optimization data, reaction scope, and mechanistic aspects to bring forward specific reactivity and selectivity trends of allylsilane in photoredox conditions.
32.	An encyclopedic compendium on chemosensing supramolecular metal-organic gels **A Sharma,** N Kaur, **N Singh** - Chemistry: An Asian journal, 2024 **Abstract:** Chemosensing, an interdisciplinary scientific domain, plays a pivotal role ranging from environmental monitoring to healthcare diagnostics and (inter)national security. Metal-organic gels (MOGs) are recognized for their stability, selectivity, and responsiveness, making them valuable for chemosensing applications. Researchers have explored the development of MOGs based on different metal ions and ligands, allowing for tailored properties and sensitivities, and have even demonstrated their applications as portable sensors such as paper-based test strips for practical use. Herein, several studies related to MOGs development and their applications in the chemosensing field via UV-visible or luminance along with electrochemical based are presented. These papers explored MOGs as versatile materials with their use in sensing bio or environmental analytes. This review provides a foundational understanding of key concepts, methodologies, and recent advancements in this field, fostering the scientific community.
33.	An evaluation of the xenobotic cognitive project: Towards stage 1 of xenobotic cognition **R Joy** - Endeavour, 2024 Abstract: Xenobot, the world's first biological robot, puts numerous philosophical riddles before us. One among them pertains to the cognitive status of these entities. Are these biological robots cognitive? To evaluate the cognitive status of xenobots and to resolve the puzzle of a single mind emerging from smaller sub-units, in this article, I juxtapose the cognitive capacities of xenobots with that of two other minimal models of cognition, i.e., basal cognition and nonliving active matter cognition. Further, the article underlines the essential cognitive capabilities that xenobots need to achieve to enter what I call stage 1 of xenobotic cognition. Stage 1 is characterized by numerous cognitive mechanisms, which are integral for the survival and cognition of basal organisms. Finally, I suggest that developing xenobots that can reach Stage 1 can help us achieve sophistication in the areas of evolution of the human mind, robotics, biology and medicine, and artificial intelligence (AI).
34.	Analysing heavy metal contamination in groundwater in the vicinity of mumbai's landfill sites: An in-depth study A Gani, A Hussain, **S Pathak**… - Topics in Catalysis, 2024 **Abstract:** The health of the public and environment may suffer significantly when solid waste is dumped in unmanaged landfills. The primary concern is the risk of pollution caused by leachate from landfill sites migrating into surface waters, & groundwater. In India, handling the leachates from landfills is a significant environmental and financial issue. Owing to the rapid urbanization, industrialization, and population increase, a variety of by-products are produced from day-to-day living and are frequently disposed of carelessly, creating serious environmental issues. This study evaluates the environmental risks to groundwater that leachate from municipal solid waste landfills poses. In order to assess the degree and kind of groundwater contamination, the research uses a thorough analytical methodology that integrates hydrogeological, geochemical, and microbiological examinations. To ascertain the physicochemical characteristics of leachate, including heavy metal concentrations, three landfill sites in Deonar, Mulund, and Malad were chosen. Landfill leachate samples were taken from three municipal solid waste (MSW) landfills and examined for 22 trace contaminants that are frequently found in surface and municipal wastewater effluents. It was discovered that the Deonar dump site was far more polluted than the

	Malad and Mulund garbage sites. The leachate pollution index was used to assess the toxicity hazard of the dumpsites; values of 20.41, 23.42, and 23.52 were found for the landfill sites in Mulund, Malad, and Deonar, respectively. This study will provide valuable insights into the present state of groundwater contamination around Mumbai landfills. Furthermore, by identifying the precise contaminants causing groundwater degradation, thorough research will facilitate the development of tailored mitigation plans. The study's findings are anticipated to have a significant impact on urban planning and policy decisions about sustainable waste management techniques, with a particular focus on groundwater resource conservation and public health in Mumbai.
35.	Analytical solution to transversely isotropic hollow cylinder under axisymmetric surface loading using variational principle **AV Sirsat, SS Padhee** - Journal of Engineering Mechanics, 2024 **Abstract:** The behavior of axisymmetric cylinders under various surface loading has remained the topic of research for many years. Most of the solutions presented in the literature are load-specific. Therefore a general solution is sought to satisfy any boundary conditions prescribed on any surface. This paper presents a general solution to satisfy a wide combination of boundary conditions prescribed on the curved as well as on the flat ends of a cylinder. A hollow cylinder was considered, composed of transversely isotropic material. The formulation is based on the variational principle, resulting in a set of coupled governing equations and associated boundary conditions. The solutions to the coupled governing partial differential equations are obtained by systematically decoupling them, followed by the method of separation of variables and the Frobenius method. All the boundary conditions are satisfied by making use of either the Fourier or the Fourier-Bessel transformation. The solutions for various test cases were validated by comparing them against three-dimensional solutions obtained using finite-element analysis. The solution for the solid cylinder was obtained by considering the limiting case of the internal radius approaching Zero.
36.	Anisotropy-assisted thermodynamic advantage of a local-spin quantum thermal machine **C Purkait**, S Chand, **A Biswas** - Physical Review E, 2024 **Abstract:** We study quantum Otto thermal machines with a two-spin working system coupled by anisotropic interaction. Depending on the choice of different parameters, the quantum Otto cycle can function as different thermal machines, including a heat engine, refrigerator, accelerator, and heater. We aim to investigate how the anisotropy plays a fundamental role in the performance of the quantum Otto engine (QOE) operating in different timescales. We find that while the engine's efficiency increases with the increase in anisotropy for the quasistatic operation, quantum internal friction and incomplete thermalization degrade the performance in a finite-time cycle. Further, we study the quantum heat engine (QHE) with one of the spins (local spin) as the working system. We show that the efficiency of such an engine can surpass the standard quantum Otto limit, along with maximum power, thanks to the anisotropy. This can be attributed to quantum interference effects. We demonstrate that the enhanced performance of a local-spin QHE originates from the same interference effects, as in a measurement-based QOE for their finite-time operation.
37.	Annual velocities of the ablation zone of Panchi Nala Glacier, western Himalaya: Trends and controlling factors PK Garg, M Prajapati, A Shukla, **S Guha…** - Polar Science, 2024 **Abstract:** Information on the glacier velocity is imperative to understand the glacier ice volume, supraglacial feature evolution and glacier-climate interaction. The present study investigates annual velocities of the ablation zone (~4500–4800 m asl) of Panchi Nala Glacier, western Himalaya through feature tracking. For this, multi-temporal Landsat (TM and OLI) and Sentinel −2 MSI images, acquired between 2000 and 2021, were correlated using the Co-registration of

	Optically Sensed Images and Correlation (COSI-Corr) tool. Results reveal a mean velocity of the ablation zone to be 10.6 ± 5.6 m/y during 2000–2021, with the highest (13.8 ± 4.6 m/y) and lowest velocity (8.9 ± 2.8 m/y) observed in 2005 and 2015, respectively. There is no significant trend in the velocity, rather it is highly heterogeneous on the inter-annual scale. Further, the influence of several factors such as slope, debris cover, altitude, annual average temperature and precipitation on the glacier velocity was investigated. Results indicate that the inter-annual heterogeneity in velocity is inversely correlated with the variation of summer precipitation implying that an increase in summer precipitation decreases the glacier velocity. The spatio-temporal velocity variations are also linked with the presence of supraglacial ponds, ice cliffs and heterogeneous debris distribution over the glacier. Findings indicate that, though annual glacier velocities have not changed significantly, their magnitudes are consistently low which coupled with consistent debris increase (19.74%) and gentle slope (8.2° over ablation zone) can promote rapid growth of supraglacial ponds and ice cliffs.
38.	Computational and experimental assessment of peacock feather AI Ansari, NA Sheikh, **N Kumar**- International Journal on Interactive Design and Manufacturing (IJIDeM), 2024 **Abstract:** Beauty attracts People and peacock feathers have got such vibrant beauty because of their colorful appearance, aesthetic appeal, and monetary value. Due to their incredible ability to transform and attract the opposite gender, peacock feathers have acquired impressively attractive qualities over hundreds of years, including the potential to attack and prey. A peacock's feather is robust enough to withstand aerodynamic stresses, maintain its aerodynamic shape, and be raised to attract the opposing gender or to defend oneself from an intruder. Additionally, it is sufficiently flexible and therefore more durable being compressed, maintaining its fractures. The study of novel bio-inspired designs on bird structure has already been reported in the literature and demonstrated the superior compressive performance of bird's feather-inspired designs; however, the Micro-CT based simulation of peacock calamus shaft and experimental comparison of compression and flexural properties using a three-point bending test has not yet published in the literature. This study examined the variance in barb length throughout the rachis as well as the barbs' tensile characteristics at three different rachis locations. In addition to this research, a micro-CT-based computer model of a peacock calamus shaft was developed to forecast the microscopic elastic and strength properties, and the outcomes of the simulation and experiment were compared. The study is divided into two parts: the first to examines the compression and three-point bending in relation to design variables obtained through post-processing of Micro-CT images, and the second to conducts an experimental investigation using the same sample of calamus shaft used for Micro-CT imaging and compares the outcomes of the two approaches. The findings of this study demonstrate that a natural feather's shaft is superior in design and it is optimized, and that Micro-CT based FEA provides good correlated results that can be utilized to predict the sample's attributes.
39.	Convergence and contrast: An investigation into the psychological attributes of budding entrepreneurs **P Singh, A Mishra** - Journal of the Knowledge Economy, 2024 **Abstract:** While promoting entrepreneurship to address unemployment among educated youth, states have predominantly emphasized physical resources, neglecting the crucial focus on psychological attributes, especially in India. Entrepreneurial intention (EI) is acknowledged as a vital psychological factor in entrepreneurial behavior, but previous research has primarily examined EI among students, leaving a gap in understanding its dynamics among a more relevant sample—entrepreneurs or aspiring entrepreneurs. Motivated by this gap, the present study explores the association of psychological attributes influencing EI in budding entrepreneurs and examines the differences in attributes between budding entrepreneurs and students not inclined towards entrepreneurship. This cross-sectional study included a sample of 83 budding

	entrepreneurs and 769 students (not inclined towards entrepreneurship) selected from various engineering colleges in Punjab, India. The study used standardized questionnaires to measure various attributes of interest such as EI, entrepreneurial self-efficacy (ESE), emotional intelligence, cognitive flexibility, internal locus of control, risk-propensity (RP), conscientiousness, and mindset. The collected data underwent analysis through correlation, t-tests, and regression analysis. The results revealed a significant association of EI with all identified variables among budding entrepreneurs. However, differences in mean scores between budding entrepreneurs and students were observed only on questionnaires related to RP, ESE, EI, and prevention-focus. In regression analysis, taking RP, ESE, and prevention focus as predictors of EI, the results revealed that 38% of the variance in EI could be attributed to these factors, with ESE emerging as the most significant predictor. This study underscores the importance of fostering ESE among students, suggesting its significant contribution to the development of higher EI. Policymakers in the field of entrepreneurship promotion may find these outcomes valuable, explore them further, and advocate for interventions targeting ESE among students.
40.	Copper-catalyzed chemoselective o-arylation of oxindoles: access to cyclic aryl carboxyimidates PR Singh, M Lamba, **A Goswami** - The Journal of Organic Chemistry, 2024 Abstract: We have developed a highly efficient base- and additive-free chemoselective CuO-catalyzed strategy for the O-arylation of 2-oxindoles to synthesize 2-phenoxy-3H-indole and 2-phenoxy-1H-indole derivatives in the presence of diaryl iodonium salts. This method offers a variety of O-arylated oxindoles in good to excellent yields under relatively milder reaction conditions. Furthermore, this methodology was extended for the O-arylation of 2-pyridinone and isoindoline-1-one derivatives as well. 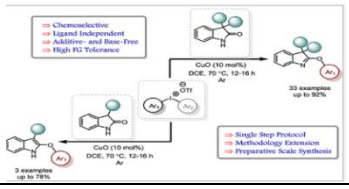
41.	ECMAC: Edge-assisted cluster-based mac protocol in software-defined vehicular networks Y Shen, J Jeong, **J Jun**, T Oh, Y Baek - IEEE Transactions on Vehicular Technology, 2024 **Abstract:** Vehicular networks have emerged as a promising means to mitigate safety hazards in modern transportation systems. On highways, emergency situations associated with vehicles necessitate a reliable media access control (MAC) protocol that can provide timely warnings of possible vehicle collisions. In this paper, we present an edge-assisted cluster-based MAC protocol (ECMAC) for packet dissemination in software-defined vehicular networks. To reduce the control messaging overhead for clustering, ECMAC separates the cluster control plane (i.e., managing cluster formation) from the data plane (i.e., actual data transmission and forwarding) by using a software-defined network controller in a cellular network edge server. For transmitting packets, we design a time-division multiple access (TDMA) schedule algorithm to guarantee a high reliability and a low latency. The TDMA schedule in ECMAC is determined by a joint optimization process in the cellular edge, which is formulated as a binary integer linear programming problem and solved by a heuristic approach based on the divide-and-conquer paradigm. This joint optimization process minimizes the signal interference by jointly considering channel assignment and time slot allocation, thereby ensuring reliable communication. Through extensive simulations, our performance results show that ECMAC improves the successful delivery ratio of emergency packets by at least 25 %, compared with state-of-the-art approaches.
42.	Effect of inhomogeneous ageing of insulation on electric field distribution of a 220kV HVAC in-service cable **P Pandey, CC Reddy** - IEEE Transactions on Dielectrics and Electrical Insulation, 2024

	Abstract: This paper primarily discusses about the phenomenon of inhomogeneous ageing observed in a 220 kV in-service HVAC cable. The XLPE layer is peeled out circumferentially using a special lathe. The samples are subjected to various material characterization tests including Fourier transform infrared spectroscopy (FTIR), X-ray diffraction (XRD), differential scanning calorimetry (DSC) and dielectric spectroscopy. The results show significant differences in morphology among XLPE layers, which is in turn reflected in permittivity measurements. The local changes in permittivity is expressed mathematically to vary along the radial position and is fitted with the experimental data. The fitted equations is used to estimate the electric field distribution inside the insulation bulk using a finite element method (FEM) software. The simulation results are also verified analytically. When compared to conventional field distribution with bulk consideration of permittivity and permittivity at radial position, a significant enhancement in electric field in the middle part of cable insulation is observed. The Field Enhancement is visualized with different accelerated ageing permittivity data from the literature.
43.	Effect of process parameters on bend angle during underwater laser bending of SS304 sheet **R Yadav, R Kant -** Lasers in Manufacturing and Materials Processing, 2024 **Abstract:** Laser bending has gained significant attention in recent years due to its advantages in accuracy, processing time, controllability, flexibility, and the ability to fabricate complex shapes. However, its application in underwater environments remains relatively unexplored. This research article presents an experimental analysis of underwater laser bending on stainless-steel sheets, focusing on the impact of different process parameters such as laser power, scanning speed, beam diameter, and water height above the worksheet surface. The bend angle found to be increased with laser power and reduced with the increasing in water height. The scanning speed and beam diameter initially increased the bend angle and started reducing after getting a peak. A significant bend angle of upto 14 degrees is achieved in the underwater condition. This study provides valuable insights into the underwater laser bending process and its sensitivity to different process conditions. The findings contribute to the understanding of the bending behavior of submerged stainless-steel sheets. Further research in this area holds great potential for advancing the capabilities of laser bending in underwater environments and expanding its range of applications in diverse industries.
44.	Electrochemical oxidative C–C bond cleavage of methylenecyclopropanes with alcohols **R Kumar, S Dutt, P Banerjee** - Chemical Communication, 2024 **Abstract:** Herein, an electrochemical approach toward the ring opening functionalization of methylenecyclopropanes (MCPs) via C–C bond cleavage in the presence of alcohols is reported. The methodology avoids the usage of external oxidants and shows good functional group tolerance. The mechanistic studies suggest that the reaction proceeds via direct single electron oxidation of the C–C bond of MCPs followed by ring opening to form the desired product.
45.	Energizing an IoT sensor using regenerative opposite fringing fields from an embedded communicating patch antenna **S Kumar, M Kumar, A Sharma,** IJG Zuazola - IEEE Access, 2024 **Abstract:** An integrated, miniature, dual-purpose circular patch antenna is proposed for Simultaneous Wireless Information and Power Transmission (SWIPT). The design proposes a proximity-coupled feed to the radiative circular patch for Wireless Information Transfer (WIT) in {mathrm {5.7 text {GHz}}} - {mathrm {6.0 text {GHz}}} band and an integrated capacitive-coupled feeding network, with full-wave rectification (FWR) using regenerative opposite fringing fields from the radiating edges of the patch for energizing IoT sensors by means of wireless power transfer (WPT) at {mathrm {5.2 text {GHz}}}. For the realization, two co-polarized fringing field harvesters are capacitively coupled to the radiating edges of the patch to regenerate those opposite fringes whose currents are effectively matched to the FWR using a pair

	of Schottky diodes for direct current (DC) power generation. Since the gain and efficiency of the patch, in WIT mode, are favoured when using the FWR network, the effective regenerative fields, which are deemed attractive in modern wireless sensor network (WSN) applications for boosting the lifespan of sensor nodes. 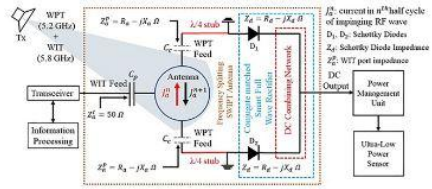
46.	Experimental investigation of single spark μ-EDM using electrodes fabricated with μ-turning process **V Ghai,** A Rathod, P Ranjan, **H Singh** - Sādhanā, 2024 **Abstract:** Micro electrical discharge machining (μ-EDM) stands out as a widely employed non-traditional machining process with diverse applications in microfluidics, electronics, medical, aeronautics, and the automotive industry. This study is dedicated to the exploration of the single spark μ-EDM process utilizing a titanium tool electrode fabricated using a μm-turning process. Intriguingly, it is established that achieving a single spark necessitates a minimum tool diameter of 8 μm. Further, the effect of critical parameters such as voltage and capacitance on material removal rate (MRR), tool wear rate (TWR), as well as the shape and size of the resultant craters is investigated. A 7 μm tool electrode when subjected to a voltage of 100 V and a capacitance of 33 pF manifests a remarkably refined surface finish, demonstrating controlled erosion on the workpiece surface. The study also indicates that MRR and TWR vary exponentially with supplied discharge energy. This comprehensive analysis not only identifies optimal conditions for μm turning during tool fabrication but also elucidates the prerequisites for generating a controlled single spark during workpiece erosion. In essence, the findings presented here contribute valuable insights to the advancement of precision μ-EDM processes.
47.	Exploring the influence of nanocrystalline structure and aluminum content on high-temperature oxidation behavior of Fe-Cr-Al alloys **R Kumar**, R.K. S Raman, S.R. Bakshi, V.S. Raja… - Materials, 2024 **Abstract:** The present study examines the high-temperature (500–800 °C) oxidation behavior of Fe-10Cr-(3,5) Al alloys and studies the effect of nanocrystalline structure and Al content on their resistance to oxidation. The nanocrystalline (NC) alloy powder was synthesized via planetary ball milling. The prepared NC alloy powder was consolidated using spark plasma sintering to form NC alloys. Subsequently, an annealing of the NC alloys was performed to transform them into microcrystalline (MC) alloys. It was observed that the NC alloys exhibit superior resistance to oxidation compared to their MC counterparts at high temperatures. The superior resistance to oxidation of the NC alloys is attributed to their considerably finer grain size, which enhances the diffusion of those elements to the metal–oxide interface that forms the protective oxide layer. Conversely, the coarser grain size in MC alloys limits the diffusion of the oxide-forming components. Furthermore, the Fe-10Cr-5Al alloy showed greater resistance to oxidation than the Fe-10Cr-3Al alloy.
48.	Fabrication of drug-loaded graded porous Ti6Al4V structures for load-bearing biomedical applications M Singh, AS Gill, PK Deol, **A Agrawal** - Journal of Materials Research, 2024 **Abstract:** The present study investigated drug-loaded, titanium alloy (Ti6Al4V) graded porous structure with desired mechanical properties for implant-based local drug delivery application. The fabricated graded porous metallic structures displayed compressive yield strength in a range of 110.8–283.8 MPa, open porosity 30.2–69.4% and Young's modulus 2.2–12.1 GPa. These

	characteristics resemble the range for human bone tissue. The electrochemical corrosion behaviour of the fabricated structures was found satisfactory even though comparatively higher corrosion rate was observed in porous samples. The analysis showed the formation of protective passive layer on the exposed surface of the porous samples. The micrographs confirmed the presence of well-distributed interconnected pores in the peripheral region of the samples which were used to load drug (simvastatin) using different dispersion media. It was found that by varying the later, the in vitro release of loaded drug can be prolonged to as long as 14 days.
49.	Facile synthesis of a three-dimensional Ln-MOF@FCNT composite for the fabrication of a symmetric supercapacitor device with ultra-high energy density: overcoming the energy storage barrier M Y Khan, **A Husain, DK Mahajan** - Dalton Transactions, 2024 **Abstract:** In order to quench the thirst for efficient energy storage devices, a novel praseodymium-based state-of-the-art three-dimensional metal–organic framework (MOF), {[Pr(pdc)2]Me2NH2}n (YK-1), has been synthesized by using a simple solvothermal method employing a readily available ligand. YK-1 was characterised by single-crystal XRD and crystallographic analysis. The electrochemical measurements of YK-1 show that it exhibits a specific capacitance of 363.5 F g−1 at a current density of 1.5 A g−1 with 83.8% retention after 5000 cycles. In order to enhance its electrochemical performance for practical application, two composites of YK-1 with graphene oxide (GO) and functionalised multi-walled carbon nanotubes (FCNTs), namely YK-1@GO and YK-1@FCNT, were fabricated by employing a facile ultrasonication technique. The as-synthesized MOF and the composites were characterized by PXRD, FTIR, SEM, and TEM techniques. YK-1@GO and YK-1@FCNT offer enhanced specific capacitances of 488.2 F g−1 and 730.2 F g−1 at the same current density with 93.8% and 97.7% capacity retention after 5000 cycles, respectively (at 16 A g−1). Fascinated by the outstanding results shown by YK-1@FCNT, a symmetric supercapacitor device (SSC) based on it was fabricated. The assembled SSC achieved a remarkable energy density (87.6 W h kg−1) and power density (750.2 W kg−1) at a current density of 1 A g−1, along with very good cycling stability of 91.4% even after 5000 GCD cycles. The SSC device was able to power up several LED lights and even operated a DC brushless fan for a significant amount of time. To the best of our knowledge, the assembled SSC device exhibits the highest energy density among the MOF composite-based SSCs reported so far.
50.	Forecasting future groundwater recharge from rainfall under different climate change scenarios using comparative analysis of deep learning and ensemble learning techniques **D Banerjee, S Ganguly,** S Kushwaha - Water Resources Management, 2024 **Abstract:** Groundwater is the most reliable source of freshwater for household, industrial, and agricultural usage. However, anthropogenic interventions in the water cycle have disrupted sustainable groundwater management. This research aims to comprehend the future of groundwater recharge predominantly due to rainfall under changing climate. In this study, predictors of groundwater recharge such as precipitation, land use land cover (LULC), soil type, land slope, temperature, potential evapotranspiration, and aridity index (ArIn) were used for the Punjab region of India over the duration of 34 years, from 1986 to 2019. To simulate future conditions, various climate change scenarios from the CMIP6 report have been incorporated. Different Artificial Intelligence and Deep Learning models, ranging from the straightforward Linear Regression model to the intricate Extreme Gradient Booting (XGBoost), used these parameters as input. Statistical analysis of the models showed that XGBoost is most effective in predicting the groundwater recharge phenomena. Correlation studies revealed precipitation to be the primary contributor to recharge, followed by the ArIn, while soil type and slope are found to have the strongest inverse correlation. The models' resilience and performance were investigated by conducting a k-fold cross-validation analysis. The pattern of groundwater recharge is forecasted for the years 2020 to 2035 across Punjab with different climate change scenarios. The

	study demonstrates how the Punjab area is mirroring its current status around Shared Socioeconomic Pathway (SSP) 370. Groundwater level estimates confirmed its strong correlation with and dependence on groundwater recharge. The analysis is strengthened by comparing the AI-predicted groundwater recharge with the Central Ground Water Board (CGWB) Punjab's annual estimate.
51.	Gamma decay hindrance factors used in systematic configuration assignments Y P Singh, V Kumar…**K Jha**… - Physics of Particles and Nuclei Letters, 2024 **Abstract:** A simple empirical relation is proposed to correlate the K-hindrance factor with the number of quasiparticles in the state configuration. The reduced hindrance = has been empirically modified such that = , instead of = , where and are the numbers of neutron and proton quasiparticles in the state configuration. In systematics, the modified hindrance factor can be used to uniquely determine the K-isomer state configuration.
52.	High strain rate response of ABS-M30i-based 3D printed, bio-inspired, bovine bone structure AI Ansari, NA Sheikh, **N. Kumar** - Proceedings of the Institution of Mechanical Engineers, Part L: Journal of Materials: Design and Applications, 2024 **Abstract:** To investigate osteoporosis caused by aging and the dynamic behavior of male bovine trabecular bone, three age groups of male bovine trabecular bone were chosen, and micro-computed tomography (CT) analysis was performed to develop an image-based bio-inspired computer-aided design (CAD) model of the bone structure. Further experimental and computational studies were carried out to examine the rate-dependent behavior and compressive energy-absorbing capacity of the structure as a function of age. To evaluate this study, a micro-CT-based CAD model of the structure was 3D printed using ABS-M30i material and subjected to quasi-static compression (low strain rate) and high strain rate (split Hopkinson pressure bar) compression. The findings show that 3D-printed bovine structures have distinct high-rate dependence at strain rates greater than 430 s−1, as well as sensitivity to strain rate in terms of peak stress, plateau stress, and energy absorption capacity. Using rate-dependent properties, the Johnson–Cook damage plasticity model was used in computational analysis to explain the dynamic behavior of bone due to osteoporosis. Overall, there is good agreement between the numerical simulations and the experimental data, which was obtained by verifying and validating the model against the experimental results.
53.	Impact of intermittent sputtering on the ordering of triangular surface topography **Rakhi, S Sarkar** - Nuclear Instruments and Methods in Physics Research Section B: Beam Interactions with Materials and Atoms, 2024 **Abstract:** It is demonstrated that the quality of nanoscale triangular structures on Si (100) surfaces can be improved by applying intermittent ion beam sputtering. This investigation is conducted along the work of Rakhi et al. (2023), which introduces an additional physical parameter space related to intermittent sputtering. Through this approach, we have observed the minimum surface defect density associated with higher-order surface structures, particularly at t = 8 min. This can have large potential applications in modern cutting-edge technology demands of controlled growth of nanostructures, especially the low dimensional high aspect ratio nanostructures.
54.	Improved catalytic activity on transitioning from inverse to normal spinel in Zn2−xGa2xSn1−xO4: a robust bifunctional OER and HER electrocatalyst RT Parayil…**K Garg, S Mehta…TC Nagaiah** - Sustainable Energy & Fuels, 2024 **Abstract:** Water splitting by electrolysis is considered as one of the best methods for the production of hydrogen which is a clean and green fuel that can replace the existing non-renewable sources. Herein, Zn2−xGa2xSn1−xO4 with oxygen vacancies has been synthesized via a solid state method. Furthermore, the influence of oxygen vacancies on electrocatalytic

	activity is investigated systematically. The presence of oxygen vacancies has been confirmed by X-ray photoelectron spectroscopy (XPS) and positron annihilation lifetime spectroscopy (PALS) and it was found that higher oxygen vacancy concentration is present in zinc gallate. As a result, $ZnGa_2O_4$ exhibits prominent hydrogen evolution reaction (HER) achieving a current density of 20 mA cm−2 with a low overpotential of 360.0 mV and prominent oxygen evolution reaction (OER) achieving a current density of 10 mA cm−2 at an overpotential of 370.0 mV, and the voltage required for overall water splitting is 2.0 V @ 10 mA cm−2. The catalyst also exhibits good stability for up to 12 hours and it exhibited a faradaic efficiency of 92% for the OER and 95% for the HER. The role of oxygen vacancies adds multifunctionalities in these materials in terms of light emission. $ZnGa_2O_4$ has shown superior photoluminescence compared to Zn_2SnO_4 and interestingly there was also color tunability from orange to blue region going from zinc stannate to zinc gallate.
55.	In-plan distribution of peak floor acceleration demands in torsionally irregular buildings **A Jain, M Surana** - Journal of Building Engineering, 2024 **Abstract:** The precise estimation of peak floor acceleration demands is essential to ensure the seismic safety of building contents and attachments. The present study aims to investigate the distribution of the peak floor acceleration demands across the floor plan in torsionally irregular buildings. To achieve this objective, 28 mid-rise reinforced concrete buildings with torsional irregularities are analyzed under 5,600 bidirectional earthquake excitations, considering various strength ratios in buildings. A total of 2,59,200 in-structure amplification factors are estimated at multiple locations within the building plan and also at different floors. It is observed that current seismic design codes tend to underestimate the in-structure amplification factor for torsionally irregular buildings, particularly at locations distant from the center of rigidity (towards flexible frames), by up to 137% for elastic buildings, and up to 54% for moderately inelastic buildings. Even in the case of frames closer to the stiff frames, the seismic design codes underestimated the in-structure amplification factor by up to 68% for elastic buildings. It is observed that a strong relationship exists between the torsional amplification of the peak floor acceleration and displacement amplification due to building torsion at the floor of interest. The torsional amplification of peak floor acceleration is found to be approximately equal to torsional displacement amplification for the flexible frames at the floor of interest. Simplified equations are developed for their integration with existing building codes to precisely estimate the in-plan distribution of peak floor acceleration demands in torsionally irregular buildings.
56.	Insights on the mechanism of uranium removal via nanofiltration in alkalinity and salinity dominated groundwater systems **M Verma, VA Loganathan** - Water, Air, & Soil Pollution, 2024 **Abstract:**Groundwater quality of Punjab, India, is a matter of huge concern due to the presence of various toxic contaminants (e.g., uranium, selenium, and arsenic) from either geogenic or anthropogenic origins. In this study, we have evaluated the potential of nanofiltration for uranium removal from contaminated groundwater under environmentally relevant conditions. The influence of membrane material properties for uranium retention capabilities in two different nanofiltration membranes, viz., NF2 and NF500, was explored. Aqueous speciation modeling of uranium (U) representing the geochemical conditions of groundwater at U-contaminated region of Punjab, India, was performed to identify the dominant uranyl species. Laboratory experiments for uranium removal by both nanofiltration membranes were conducted using synthetic groundwater. The pure water flux of NF2 and NF500 was 24 ± 0.62 L·m2·h−1·bar−1 and 5.4 ± 0.21 L·m2·h−1·bar−1, respectively, wherein the former was 5 times higher than the latter despite NF2 having lesser molecular weight cutoff (MWCO). The uranium removal was highly dependent on the aqueous speciation influenced primarily by solution pH. Uranium rejection was maximum at neutral pH in both the membranes, with 87% and 78% rejection for NF2 and NF500, respectively. Uranium uptake by the membranes was highest at pH 7.0 with 77.10% and

	44.6% for NF2 and NF500, respectively. Membrane transport parameters, i.e., solute flux and solute permeability, indicated the prevalence of size exclusion and/or charge-based interactions operative over a range of pHs. The uptake of uranium onto the membrane was minimal at alkaline pH with the least flux decline (ca. 6.25% in NF2) that indicated low membrane fouling. Overall, our results indicate that both World Health Organization and Atomic Energy Regulatory Board (AERB) drinking water guideline values (i.e., 30 µgL−1 and 60 µgL−1) could be achieved via nanofiltration technology as U-affected regions of Punjab have the ambient groundwater pH in neutral-alkaline range. 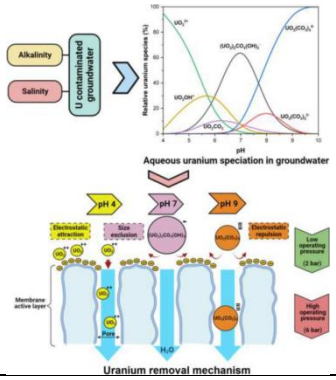
57.	Interaction of surface water waves with partial porous structure and floating elastic plate in the presence of sea wall **G Sahoo,** S Singla, **SC Martha** - Ships and Offshore Structures, 2024 **Abstract:** This study proposes a model composed of either bottom-standing porous structure (BSPS) or surface-piercing porous structure (SPPS) in combination with an elastic plate (EP) placed at a distance from one another to protect a sea wall. The study uses the governing equation and the boundary conditions to coin a system of equations, and the system of equations is solved to identify the hydrodynamics coefficients. Further, it is noticed that length, frictional coefficient, porosity of the porous structure, and flexural rigidity of EP play a crucial role in reducing the force on the sea wall, water elevation and plate deflection. The SPPS exhibits a nearly 60% reduction in wall force coefficient due to a 50% increase in wave-damping when compared to BSPS for k0H = 0.85. These results are crucial for developing floating structures that can resist harsh wave environments and minimize the effects of waves close to the shore.
58.	Investigating the role of anger and cognitive malfunction in mental health: A cross-sectional exploration paving the way for a subsequent experiment **S Kharwar, P Singh** - The Journal of Psychology, 2024 **Abstract:** The functional outcomes associated with subjective well-being (SWB) and the detrimental aspects of psychological distress (PD) make it essential to explore contributing factors. The present study investigated a model about the existing gap in the determining role of trait anger (TA), state anger (SA), cognitive reappraisal (CR), rumination and cognitive failure (CF) as predictors of SWB and PD. The study contributes by exploring the interaction of dispositional, situation factors and emotional regulation strategies in shaping SWB and PD in the Indian Sample. A cross-sectional survey design was employed wherein 600 young adults aged 18–40 (Mage = 22.13, SDage = 4.06) were recruited from Uttar Pradesh, India using a multi-level cluster sampling method. The data were collected using questionnaires in the field setting during August–December 2021. Regression and path analysis revealed that the proposed predictors explained significant variance in SWB and PD, i.e., R2 = 0.24, F (5, 594) = 38.03, p < 0.01, Cohen f2 =0.31 and R2 = 0.35, F (5, 594) = 66.40, p < 0.01, Cohen f2 = 0.53, respectively. The models also fit well with the statistical indices. Except CR, all predictors emerged as significant risk factors. The findings suggest that the interventions to reduce PD and enhance SWB may consider inculcating CR and reducing higher levels of TA, SA, rumination and CF to enhance an individual's adaptive functioning. The findings pave the way for conducting a pre-

	planned experiment to study the outcomes of various levels of TA in regulating incidental anger (SA) employing CR and rumination.
59.	Linkage among the neutron-skin thickness of 208Pb and nuclear symmetry energy using heavy particle radioactivity **M Kaur**, SK Patra, **PK Raina** -Journal of Physics G: Nuclear and Particle Physics, 2024 **Abstract:** Journal of Physics G: Nuclear and Particle Physics Purpose-led Publishing, find out more. ACCEPTED MANUSCRIPT Linkage among the neutron-skin thickness of 208Pb and nuclear symmetry energy using heavy particle radioactivity Manpreet Kaur1, S K Patra2 and P K Raina3 Accepted Manuscript online 10 April 2024 • © 2024 IOP Publishing Ltd What is an Accepted Manuscript? DOI 10.1088/1361-6471/ad3cfa DownloadAccepted Manuscript PDF Article metrics 8 Total downloads Submit Submit to this Journal Permissions Get permission to re-use this article Share this article Share this content via email Share on Facebook (opens new window) Share on Twitter (opens new window) Share on Mendeley (opens new window) Article and author information Abstract The nuclear symmetry energy (NSE) is a linchpin in deciphering the behavior of matter in a wider domain extending from the characteristics of exotic nuclei to those of neutron stars in the cosmos.
Therefore, it is crucial to utilize potential probes to constrain the NSE and its slope parameter L(ρ_{0}). In this work, we put forth the heavy particle radioactivity (HPR) as a probable bridge among the slope of NSE (L(ρ_{0})) and neutron-skin thickness of ^{208}Pb (R_{skin}^{208}), which serves to put constrain on the L(ρ_{0}) value. The NSE and its slope parameter are determined from the single nucleon potential of asymmetric nuclear matter exploiting the analytical relationship between these quantities. The isovector/symmetry potential component of the single nucleon potential is derived through HPR for varying R_{skin}^{208} by employing the heavy particle/cluster densities and core densities from the relativistic mean field model in conjunction with M3Y nucleon-nucleon interaction. It facilitates in constraining the L(ρ_{0}) value and neutron skin of finite nuclei using HPR as a linkage, where heavy cluster and core densities of standard Fermi form are considered. The constrained value of L(ρ_{o}) is 48 $\pm$ 9 MeV, which aligns with other estimations derived from nuclear mass measurements, dipole polarizability measurements and astrophysical data.
60.	Mechanical, metallurgical and corrosion analysis of forced cooling assisted laser bending of duplex-2205 R Yadav, **G Vinay, R Kant** - Optics & Laser Technology, 2024 **Abstract:** Laser bending with a small bend angle poses challenges in manufacturing applications. Despite various proposed strategies, the achievable bend angle typically ranges from 0.1 to 2° per scan. This study focuses on enhancing the bend angle of duplex stainless steel by introducing forced cooling (FC). The application of FC aims to reduce the number of scans required, thereby saving time, cost, energy, and controlling material degradation due to excessive heating. The investigation compares the effects of process parameters under natural cooling (NC) and FC conditions. Metallurgical, mechanical, and corrosion properties of the bent specimens are investigated. Results indicate a significant enhancement in the bend angle with FC, showing an improvement of up to 1592 % for specific parameters and sheet geometries. For a 2 mm sheet thickness, the maximum bend angles achieved in five scans are 14.02° and 22.34° under NC and FC conditions, respectively. The influence of process parameters on the bend angle is significantly affected by FC compared to the NC condition. Additionally, the trend of bend angle increment in each scan is almost opposite in FC condition compared to NC. FC results in increased hardness and tensile strength of the bent specimens at the expense of ductility. Microstructural analysis reveals phase rearrangement and grain refinement. Corrosion resistance remains mostly unaffected, although a slight reduction in pitting potential is observed under FC, which is compensated by the formation of a passivation layer. Interestingly, the bend angle achieved in one scan was up to three times higher than the published literature, which could be

	beneficial for various industries.
61.	[Modified isotropic and kinematic hardening equations for 304L SS under low cycle fatigue] **N Mehani, S C Roy** - Computational Materials Science, 2024 **Abstract:** This article simulates the low cycle fatigue behavior of 304L SS that exhibited initial hardening, softening, saturation, and significant secondary hardening. The combined non-linear isotropic and kinematic hardening model has been modified, implemented in ABAQUS, and validated with experimental results. New non-dimensional functions were introduced in the constitutive laws such that both isotropic and kinematic hardening behaviors depend on the accumulated plastic strain and maximum plastic strain range memory. The proposed isotropic hardening equation additively decomposes the cyclic hardening behavior into hardening, softening, and secondary hardening parts and captures the cyclic peak stress variation throughout the fatigue life well. Fatigue life is well predicted from the simulated loops. 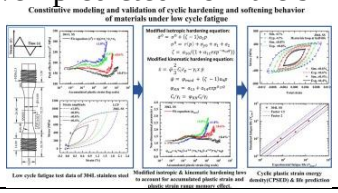
62.	[Multichannel two-dimensional MoS2 nanosheet MOSFET for future technology node] **A Rawat, B Rawat** - IEEE Transactions on Electron Devices, 2024 **Abstract:** In this work, we explore the 3-D integration of single layer (SL) and bilayer (BL) MoS Undefined control sequence \textsubscript in stacked gate-all-around (GAA) nanosheet field-effect transistor (NS-FET) using fully calibrated TCAD simulation for the future technology node. Our research primarily focuses on a comparative analysis between multichannel stacked SL-and BL-MoS Undefined control sequence \textsubscript NS-FETs with various-width Si NS-FETs, which show that BL-MoS Undefined control sequence \textsubscript NS-FET outperforms its Si NS-FET counterpart for sub-5-nm technology nodes. The results show that the vertical stacking of SL-and BL-MoS Undefined control sequence \textsubscript NS-FET significantly enhances the switching performance metrics and provides strong immunity against short-channel effects at aggressively scaled technology nodes over 50-nm wide Si NS-FET counterpart. On the other hand, the Schottky barrier (SB)-type contact with MoS Undefined control sequence \textsubscript NS-FETs is found to have inferior ON-state and OFF-state characteristics compared to doped-type contacts. Moreover, the CMOS inverter based on BL-MoS Undefined control sequence \textsubscript demonstrates the potential for lower power consumption at iso-frequency and higher operating frequency at iso-power compared to SL-MoS Undefined control sequence \textsubscript and Si NS-FETs. Our research underscores that MoS Undefined control sequence \textsubscript with stacked NS-FETs offers a promising solution for advancing technology nodes to 1 nm and beyond.
63.	[Nanopatterning induced Si doping in amorphous Ga2O3 for enhanced electrical properties and ultra-fast photodetection] **D Kaur, Rakhi, R Posti, J Singh, D Roy, S Sarkar, M Kumar** - Small, 2024 **Abstract:** Ga_2O_3 has emerged as a promising material for the wide-bandgap industry aiming at devices beyond the limits of conventional silicon. Amorphous Ga_2O_3 is widely being used for flexible electronics, but suffers from very high resistivity. Conventional methods of doping like ion implantation require high temperatures post-processing, thereby limiting their use. Herein, an unconventional method of doping Ga_2O_3 films with Si, thereby enhancing its electrical properties, is reported. Ion-beam sputtering (500 eV Ar^+) is utilized to nanopattern SiO_2-coated Si substrate leaving the topmost part rich in elemental Si. This helps in enhancing the carrier conduction by increasing *n*-type doping of the subsequently coated 5 nm amorphous Ga_2O_3 films, corroborated by room-temperature resistivity measurement and valence band spectra,

	respectively, while the nanopatterns formed help in better light management. Finally, as proof of concept, metal-semiconductor-metal (MSM) photoconductor devices fabricated on doped, rippled films show superior properties with responsivity increasing from 6 to 433 mA W^{-1} while having fast detection speeds of 861 µs/710 µs (rise/fall time) as opposed to non-rippled devices (377 ms/392 ms). The results demonstrate a facile, cost-effective, and large-area method to dope amorphous Ga_2O_3 films in a bottom-up approach which may be employed for increasing the electrical conductivity of other amorphous oxide semiconductors as well.
64.	Optical nonlinearities and applications of ZnS phosphors A Chauhan, R Sharma, M Singh, **R Sharma** - Advanced Optical Technologies, 2024 **Abstract:** Optical nonlinearities play a crucial role in enabling efficient and ultrafast switching applications that are essential for next-generation photonic devices. ZnS phosphor material produces the best results in terms of increased luminescence quantum yield when doped with certain impurities. Nevertheless, the investigation of the third-order nonlinear optical susceptibility of the phosphor materials can be exploited for various switching applications. In this regard, we review the recent advancements in the investigation of nonlinear optical properties of ZnS phosphors, where the knowledge of absorption and refraction is utilized in various optical and detector applications. Furthermore, the review highlights strategies employed to enhance the nonlinear optical response of phosphor materials as well as a general discussion of an attosecond optical switching scheme which can be used to fabricate devices with petahertz speeds. Consequently, we provide a solution to the unsolved problem of the significant extension of optical limiting applications to switching applications by developing design strategies to manipulate conventional ZnS phosphor material. The potential challenges and future prospects of utilizing phosphor materials for switching applications are also addressed. The strategies for manipulating ZnS phosphor can be generalized for a broad range of other materials by minimizing linear and nonlinear losses, while enhancing the values of the nonlinear refractive index coefficient. We propose that the figure-of-merit of ZnS material can be enhanced by using a suitable combination of pump and probe wavelength values, which can be useful for optical switching applications.
65.	Optimization techniques for IDS-Generated traffic congestion control in VANET Y Kumar, V Kumar, **B Subba** - Internet Technology Letters, 2024 **Abstract:** Vehicular Ad-hoc Network (VANET) is an emerging field of wireless networks that enables a variety of vehicle safety and convenience applications. It employs Intrusion Detection System (IDS) frameworks in its different tiers to ensure reliable and secure communication among nodes. However, IDS requires a significant amount of data to process for monitoring intrusive activities in the network. As a result, the volume of traffic increases, resulting in the network congestion. Motivated by this fact, this study provides an overview of the optimization techniques for VANET traffic congestion control. It discusses a state-of-the-art analysis along with the requirements for IDS-generated traffic congestion control. It highlights the congestion control approaches for the traffic generated by an IDS and identifies the challenges in this domain. This study also proposes a novel IDS framework for reducing IDS-generated network traffic by combining the Local Outlier Factor and Random Forest classifier. The proposed study achieved a high precision while yielding low false positive and false negative rates. The study outperformed the existing studies with an increase in accuracy of 1.16% and a reduction in attack detection time of 1.1869 seconds. Additionally, it discusses the possible future research directions that can be applied to address the issues of IDS-generated traffic congestion. Overall, this study serves as a comprehensive guide to the current status of IDS-generated traffic congestion control and diverse approaches to lessen it that can be employed by academicians and researchers.
66.	Origin of near-failure in Au contacts to polycrystalline β-Ga2O3 at high temperatures using interfacial studies **D Kaur, R Dahiya, S Shivani, M Kumar** - Applied Physics Letters, 2024

	Abstract: Suitable contacts to gallium oxide are a controversial topic with contact behavior depending heavily on the pre- and post-processing conditions. Especially for the extreme environment applications such as those involving high temperatures, contact chemistry is varied and severely lacks understanding. Herein, we report on conventional pure Au contacts to polycrystalline β-Ga2O3, used as Schottky contacts, and explore the origin of their near-failure at high temperature up to 850 °C. For this purpose, β-Ga2O3 with Au interdigitated electrodes is subjected to high temperature annealing and their interface chemistry is studied and correlated with device performance for solar-blind photodetection. Around the optimized temperature of 450 °C, the performance of the PDs is found to be maximum, whereas it reduces drastically at 850 °C. Physical damage to the electrodes along with the formation of intermetallic gold-gallium alloy is observed via XPS depth profile studies and found to be the reason for the near-failure of device at extreme conditions. Although the alloy formation begins to slightly appear at 650 °C and reduces the performance, still it does not lead to device breakdown. This study proves that unlike its counterparts GaN and GaAs, which have reported alloy formation at lower temperatures, β-Ga2O3 shows a higher resilience to the formation of Au–Ga alloy and can withstand higher temperatures before the actual device failure is reached. The proposed study shows the stability of standard metal contacts to Ga2O3 based devices, which have far-reaching implications for the future commercialization of wideband gap semiconductor based (opto)electronics.
67.	Prolonged pattern coarsening in ion irradiated swinging Si substrates **Rakhi, S Sarkar** - Vacuum, 2024 **Abstract**: Low energy ion beams are regarded as an effective means to spatio-temporally pattern a wide variety of surfaces that exhibit intriguing motifs. In this work, an unconventional technique of surface patterning has been demonstrated by studying the topographical evolution of a Si(100) surface in the presence of azimuthal sample swinging ( ) under 500 eV Ar irradiation with a polar incidence angle of 67°. A prolonged wavelength coarsening is also noticed for the swinging sample. Ripple anticoarsening is observed for static sample at high fluences. The linear and nonlinear growth regimes are found to bear a direct consequence of this unconventional geometry. Furthermore, two-dimensional slope distributions of the surface morphologies clearly indicate reduced asymmetries in the surface structures. The present geometry brings in an additional factor of differential exposure and redeposition effects in addition to the near-surface mass redistribution, the former being inconceivable in the static configuration. This study establishes the role of this unconventional yet simple method to precisely modify and control surface asymmetries and influence regime shifts.
68.	Reversible hydrogen storage in a superalkali nli4-decorated biphenylene monolayer: Insights from a first-principles study **P Beniwal, P Gautam, N Duhan, TJ Dhilip Kumar** - ACS Applied Energy Materials, 2024 **Abstract:** Hydrogen (H2) energy has been recognized as a prominent choice for sustainable green energy applications. The primary obstacle lies in its storage, emphasizing the need for an efficient storage medium. Taking this into consideration and utilizing first-principles density functional theory, we conducted an extensive study to explore the H2 adsorption potential of the biphenylene (BPN) monolayer decorated with superalkali NLi4 clusters. The NLi4 cluster exhibits a binding energy of −3.21 eV/NLi4, when positioned on both sides of the BPN. The cluster binds to the BPN monolayer via an electronic charge transfer mechanism, leading to the creation of a positive charge on the Li atoms, which facilitates the polarized H2 adsorption through electrostatic and van der Waals interactions. Under maximum hydrogenation, the 2NLi4@BPN complex can adsorb 24 H2 molecules with a gravimetric density of 11.5 wt %, surpassing the latest criterion of the Department of Energy, 5.5 wt %. Ab initio molecular

	dynamics simulations at 300 K unveil H2 reversibility and the thermal stability of the 2NLi4@BPN complex. Thermodynamic analysis and desorption temperature studies reveal the feasibility of reversible H2 storage under ambient conditions. The energetics and high gravimetric density of NLi4-decorated BPN make it a prospective material for reversible hydrogen storage.
69.	RSPP: Restricted static pseudo-partitioning for mitigation of cross-core covert channel attacks **J Kaur, S Das** - ACM Transactions on Design Automation of Electronic Systems, 2024 **Abstract:** Cache timing channel attacks exploit the inherent properties of cache memories: hit and miss time along with the shared nature of the cache to leak secret information. The side channel and covert channel are the two well-known cache timing channel attacks. In this article, we propose Restricted Static Pseudo-Partitioning (RSPP), an effective partition-based mitigation mechanism that restricts the cache access of only the adversaries involved in the attack. It has an insignificant impact of only 1% in performance, as the benign processes have access to the full cache and restrictions are limited only to the suspicious processes and cache sets. It can be implemented with a maximum storage overhead of 1.45% of the total Last-Level Cache (LLC) size. This article presents three variations of the proposed attack mitigation mechanism: RSPP, simplified-RSPP (S-RSPP) and corewise-RSPP (C-RSPP) with different hardware overheads. A full system simulator is used for evaluating the performance impact of RSPP. A detailed experimental analysis with different LLC and attack parameters is also discussed. RSPP is also compared with the existing defense mechanisms effective against cross-core covert channel attacks.
70.	Seismic response of rocking shallow foundation in RC framed structure: A parametric study **RM Kannan, N James, P Haldar** - Journal of Vibration Engineering & Technologies, 2024 **Abstract:** Purpose: This article concentrates on rocking foundation which is one of the most effective design alternatives to safeguard the super structure from excessive damage due to higher lateral forces during severe earthquakes. Methods: The present study aims to illustrate the beneficial effects of rocking foundations on the overall seismic performance of high-rise Reinforced Concrete (RC) frame structures by comparing with its conventionally designed foundation and fixed base counterparts. Within the OpenSees framework the rocking foundation and conventionally designed foundations are modelled as Beam on Nonlinear Winkler Foundation (BNWF) and super structure elements are modelled using fiber section approach with distributed plastic hinges. Results: Nonlinear static pushover analyses revealed that allowing rocking at the footing level increases yield and peak displacement by about 9% to 34% without significant reduction in the strength of the structures. Further, plastic displacement capacity is enhanced with increasing rocking effect, indicating the beneficial effect of foundation rocking on the overall seismic performance of the structure. Based on the results obtained from nonlinear dynamic time history analyses, it is ascertained that the moment transferred from column to foundation, owing to seismic action, decreases by 20% to 50% with a reduced peak roof acceleration and increasing settlement at the base of the foundation with increasing foundation rocking. However, the maximum settlement did not exceed permissible limits mentioned in Indian standards. From the fragility assessment, it is noticed that the increasing foundation rocking substantially reduces the collapse probability by a maximum of 10% than the fixed base counterparts for the 8-storey and 10-storey structures resting on dense and very dense sand. Conclusions: The findings from this study shows that it is desirable to under-proportion the size of footings with reduced earthquake loads by up to 50%, in order to improve the overall seismic behaviour of RC-framed structures during severe earthquake events.
71.	Selective furfural hydrodeoxygenation over Cu-Fe catalysts with In-Situ Cu@Fe3O4 formation **A Jaswal, V Garule…PP Singh, T Mondal**… - Journal of Industrial and Engineering Chemistry, 2024

	Abstract: This study investigates Cu-Fe mixed oxide catalysts with varying Cu/Fe molar ratios (0.5 to 2) synthesized via a sol–gel method for vapor-phase FFR HDO. The catalysts were characterized using XRD, H2-TPR, NH3-TPD, N2 physisorption, FESEM and XPS to gain sights into their properties. The characterizations unveiled the critical role of Cu/Fe molar ratio in influencing the properties and performance of the catalysts in FFR HDO. Fe promoted the dispersion of CuO, especially at a Cu/Fe ratio of 1, revealing synergistic Cu-Fe interactions. Increasing Cu/Fe ratio enhanced the reducibility of Fe but diminished that of Cu. Extensive investigations were conducted to assess the impact of key parameters, including Cu/Fe ratio, temperature, contact time, reduction temperature and H2/FFR molar ratio. The Cu-Fe mixed oxide catalyst with Cu/Fe = 1 proved to the optimal catalyst, exhibiting > 99 % FFR conversion and 90 % 2-MeF selectivity at H2/FFR = 15, 230 °C, and 0.5 gFFR h−1 gcatalyst -1. The extended evaluation of catalytic activity demonstrated sustained high performance, with stable conversion and 2-MeF selectivity values of > 99 % and 90 % over a period of 12 h. Even after 24 h on stream, the conversion remained above 90 %. Subsequent regeneration study showed partial recovery of the activity, with the catalyst maintaining conversion and selectivity consistently at about 85 % and 86 %, respectively for 10 h. Catalyst deactivation was a result of the site and/or pore blockage caused by the adsorption of FFR and FAL as well as the formation of oligomeric compounds on the catalyst's surface.
72.	Simultaneous nonvanishing of central L-values with large level **B Kumar**, M Manickam, KD Shankhadhar - Forum Mathematicum, 2024 **Abstract:** For a given normalized newform f of large prime level, we establish a lower bound with respect to the level for the number of normalized newforms g of the same weight and level as of f such that the central L-values of f and g both twisted by a quadratic character do not vanish.
73.	SiO2@Cu core-shell nanostructure impregnation on phase changed material (paraffin) for thermal energy storage **N Bora**, DP Joshi, **MK Adak** - Experimental Heat Transfer, 2024 **Abstract:** The present research aims to achieve a shape-stable, and leakage-proof material for thermal energy storage (TES). The leakage analysis of 20 wt.% SiO2@Cu PCM shows 0.05%, as a result, more testing is conducted to assess its morphology, structure, and thermal properties. TGA and DSC studies demonstrated that the latent heat and thermal degradation rate (TDR) has been delayed, with a significant decrease in latent heat of roughly 8.7% compared to pure paraffin. Laser Flash Method (LFA) results revealed that the thermal conductivity (TC) of the PCM composite significantly increased 4.84 times than the paraffin.
74.	Sustainable approach for machining of Ti6Al4V using micro-pillar textured turning tool insert **G Saraf, NH Sutrave, CK Nirala** - Sustainable Materials and Technologies, 2024 **Abstract:** The use of cutting fluids (CF) in metal cutting is questioned due to environmental and biological impacts, encouraging the adoption of dry machining to minimize these effects. However, dry machining accelerates tool wear, particularly in difficult-to-machine materials like Titanium and Nickel alloys. Approaches, such as rake surface texturing, address this challenge and promote sustainability in metal cutting. This study explored the impact of an innovative micro-pillar texture pattern fabricated using a combination of Laser Beam Micro Machining (LBμM) and Reverse Micro Electrical Discharge Machining (RμEDM) for the dry machining of Ti6Al4V. The investigation considers various parameters, including tool wear, contact length, titanium adhesion, cutting forces, cutting temperature, and chip morphology. An indirect approach was adopted to estimate the temperature of the tool tip using the temperature measured at a distant location. Implementing the textured tool with 15 μm deep micro-pillars in the dry machining of Ti6Al4V exhibited the best overall performance for various responses. A notable reduction of more than 40% for both tool-chip contact length and titanium adhesion, compared to

	a plain tool, indicated a perceptible decrease in the seizure zone at the interface. Moreover, the textured tools demonstrated a remarkable maximum reduction of 56.4% in flank wear, ensuring the prolonged retention of a sharp cutting edge. The responses for contact length, adhesion, and flank wear contributed to an 18.8% decrease in cutting force and a substantial 45.7% reduction in thrust force. Force analysis further confirmed the directional independence of the texture pattern. Under the influence of surface texturing, chip morphology changed to shorter, untangled, and tightly curled, with a 30.8% reduction in curl radius. A theoretical estimation based on the minimum energy approach was also performed to demonstrate an increment in the shear plane angle. 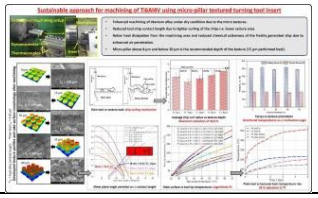
75.	Synthesis and characterization of TiO2 foam and SiO2@TiO2 core-shell nanostructure for gnetin dye degradation from industrial effluent **N Bora**, DP Joshi - Environmental Quality Management, 2024 **Abstract:** The current study intends to create TiO2 foam, SiO2 nanoparticles (NPs), and SiO2@TiO2 core-shell nanostructure (CSN) with improved photocatalytic durability for the quick degradation of the textile industrial water pollutant in the presence of sunlight. The sol-gel, Stöber, and chemical co-precipitation methods have been used to synthesize TiO2 foam, SiO2 NPs, and SiO2@TiO2 CSN. X-ray diffraction results have revealed the anatase phase of TiO2 foam, the amorphous nature of SiO2 NPs, and the amorphous nature of SiO2@TiO2 CSN due to equal wt.% of SiO2 NPs and TiO2 foam at 300 K. Field emission scanning electron microscope images show that the TiO2 foam, SiO2 NPs, and SiO2@TiO2 CSN exhibit cluster sheets, spherical, and spherical raspberry-like homogeneous morphology. The ultraviolet spectrum confirmed that the TiO2 foam and SiO2@TiO2 CSN have a band gap of 2.9 eV and 3.4 eV. SiO2@TiO2 CSN has been shown an excellent decomposition rate of water pollutants (gentian dye) in comparison to TiO2 foam due to their better-absorbing nature. Both NPs and CSN employed in the breakdown of gentian dye have been recycled and their original characteristics are preserved. The proposed SiO2@TiO2 CSN has a higher potential for application in developing self-cleaning, long-lasting, and air-purifying materials.
76.	Synthetic 18F labeled biomolecules that are selective and promising for PET imaging: Major advances and applications M Lamba, PR Singh, **A Bandyopadhyay, A Goswami** - RSC Medicinal Chemistry, 2024 **Abstract:** The concept of positron emission tomography (PET) based imaging was developed more than 40 years ago. It has been a widely adopted technique for detecting and staging numerous diseases in clinical settings, particularly cancer, neuro- and cardio-diseases. Here, we reviewed the evolution of PET and its advantages over other imaging modalities in clinical settings. Primarily, this review discusses recent advances in the synthesis of 18F radiolabeled biomolecules in light of the widely accepted performance for effective PET. The discussion particularly emphasizes the 18F-labeling chemistry of carbohydrates, lipids, amino acids, oligonucleotides, peptides, and protein molecules, which have shown promise for PET imaging in recent decades. In addition, we have deliberated on how 18F-labeled biomolecules enable the detection of metabolic changes at the cellular level and the selective imaging of gross anatomical localization via PET imaging. In the end, the review discusses the future perspective of PET imaging to control disease in clinical settings. We firmly believe that collaborative multidisciplinary research will further widen the comprehensive applications of PET approaches in the clinical management of cancer and other pathological outcomes.

77.	Temperature-induced supersolidity in spin-orbit-coupled Bose gases **Rajat, Ritu,** S Roy, **S Gautam** - Physical Review A, 2024 **Abstract:** Close to the superfluid plane-wave (PW)-supersolid stripe (ST) phase transition point of a zero-temperature quasi-one-dimensional spin-orbit-coupled Bose gas, we find that an increase in temperature induces a phase transition to the supersolid phase with a broken translational symmetry from the superfluid plane-wave phase. We use the Hartree-Fock-Bogoliubov theory with the Popov approximation to investigate the effect of thermal fluctuations on the collective excitation spectrum and investigate the softening of the spin-dipole mode corresponding to the shift in the quantum critical point. This is in stark contrast to the PW-ST phase transition in a homogeneous system where nonzero temperatures facilitate the melting of the stripe phase.
78.	The cooperative effect of Co and CoO in Co/CoO enabled efficient catalytic hydrogenation and demethoxylation of guaiacol to cyclohexanol B P Singh, G S More, R Bal, R Srivastava - Sustainable Energy and Fuels, 2024 **Abstract:** The selective catalytic transformations of lignin-derived phenolics into cyclohexanol provide an alternative renewable solution to fine-chemical industries over the fossil-fuel-dependent routes. Herein, low-cost, non-noble metal-based Co/CoO catalysts with oxygen vacancies were prepared by a simple reduction of Co3O4 at 300 °C for 20 minutes. The catalyst was utilized for the hydrogenation and demethoxylation of guaiacol, a lignin model compound, into cyclohexanol, an industrially important compound. Under relatively milder reaction conditions of 170 °C, 2 MPa H2 pressure and 2 h, 94% conversion of guaiacol with 80% cyclohexanol selectivity was obtained. The catalytic activity of Co/CoO towards hydrogenation and demethoxylation of guaiacol relied on the Co and CoO ratio, which in turn was varied through alteration in the reduction conditions of Co3O4. Metallic Co nanoparticles growth and its influence on the electronic environment of CoO in Co/CoO catalysts was confirmed using XPS, H2-TPD, NH3-TPD, and H2-TPR techniques. Several phenolics were successfully converted to corresponding cyclohexanols with the developed catalyst. The catalyst was efficiently recycled with no appreciable loss in the activity. The spent catalyst showed similar chemical environments to that of the fresh catalyst. The present work provides useful insights into the simple synthesis of an economical heterogeneous catalyst that can encourage researchers to produce other valuable chemicals and fuels from non-fossil resources under milder conditions required by the petrochemical, fine chemical, and pharmaceutical industries.
79.	The unit group of the group ring over $\mathbb{Z}n$ **H Setia**, **M Khan** - Communications in Algebra, 2024 **Abstract:** LetZnbe the ring of integers modulon.LetCt,Em,andFr,srespectivelydenote the cyclic group of ordert, the elementary abelian 2-group of order2m, and the abelian group of exponent 4 with order 2r4s. In this article, wefind the structure and generators of the unit groupV(ZnC2).Wealsosolvethenormal complement problem inV(ZnC2). Additionally, we provide a normalcomplement ofEminV(Z2nEm). At the end, we determine the structure ofV(ZpnFr,s)for an odd primepand establish thatFr,sdoes not have a normalcomplement inV(ZpnFr,s).
80.	Thermal energy storage performance of biaxial voided RCC roof slab integrated with macroencapsulated PCM for passive cooling of buildings **PJ Abass, S Muthulingam** - Journal of Energy Storage, 2024 **Abstract:** Building space heating and cooling power consumption is growing due to population and economic growth. Integrating phase change materials (PCMs) into various building envelope components is being explored to enhance thermal energy storage capacities. Specifically, roofs exposed to direct sunlight significantly promote thermal energy transfer to the interior, increasing

	the space heating and cooling requirements. In this study, thermal energy storage performance of a biaxial voided roof slab integrated with PCM is experimentally investigated under ambient conditions and compared with a normal reinforced concrete (RCC) without PCM. PCM selection, characterization, and metal void former development are performed, followed by macroencapsulation and integration into the roof slab. Thermal performance measures are evaluated, including temperature profile, heat flux, thermal load, time lag, and decrement factor. Financial viability indicators such as electricity cost savings, payback period, and CO2 emissions savings are also assessed. The results show PCM integrated biaxial voided roof slab reduces interior temperature by upto 7.2 °C during sunny hours, heat transfer to the interior by upto 60.6 %, and thermal load by upto 54 %. In addition, considering heating and cooling, it offers an average daily saving of 0.06 USD/kWh/m2 and a payback period of about 5.7 years. Further, it gives CO2 emissions savings of upto 13.7, 12.3, and 4.3 kgCO2/kWh for lignite-, coal-, and natural gas-fired power plants. Furthermore, its mean time lag is 4.2 h, with a decrement factor of 0.75 compared to 3.9 h and 0.85 for the normal RCC unit. The study makes significant contribution to knowledge by providing a unique, simple yet highly effective PCM macroencapsulation integration technique for roof slabs and insights into its thermal performance under the hot weather conditions.
81.	Tuning the plasmonic response of periodic gold nanodisk arrays for urea sensing **GP Singh**, B Fuhrmann…**N Sardana** - Journal of Materials Science, 2024 **Abstract:** Laser interference lithography (LIL) was used to fabricate gold nanodisk arrays on glass which was studied as surface-enhanced Raman spectroscopy (SERS) substrates. The Raman response of varying array periods (250 nm, 300 nm, 344 nm, 395 nm, and 446 nm) was compared using the chemical rhodamine 6G. The 300-nm period displayed the highest SERS enhancement among the tested LIL substrates. Experimental transmission measurements and their finite element method (FEM) simulations were taken to understand the optical response of the LIL substrates. The 300-nm-period LIL substrate was used to detect urea to confirm its practical use as a SERS substrate. The enhancement factor of the 300-nm-period substrate was 2.3 × 106. Furthermore, the detection limit of urea was 0.05 mM for the optimized substrate. 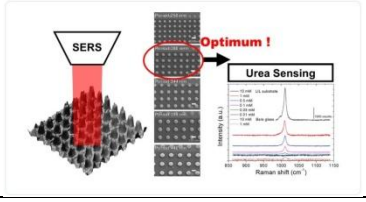
82.	Type-II superconductivity in the Dirac semimetal PdTe 2 **R Gupta**, C Witteveen, D Das… - Physical Review B, 2024 **Abstract:** We report on the microscopic superconducting properties of the Dirac semimetal PdTe 2 . In this study, we have focused on mosaic crystals of PdTe 2 , and used detailed zero-field and transverse-field muon-spin relaxation/rotation (μ SR) , ac-magnetic susceptibility, and resistivity measurements to investigate their superconducting properties. The magnetic susceptibility measurements reveal two superconducting transition temperatures at 1.8 and 1.6 K, respectively, in agreement with earlier reports. In contrary to these reports, we find that these mosaic PdTe 2 crystals are not type-I, but rather type-II superconductors. In fact, we observe the clear manifestation of a flux-line lattice through a clear diamagnetic shift and Gaussian broadening of the Fourier spectra in the superconducting state. This behavior is likely caused by the disorder in the mosaic crystals of PdTe 2 studied here. Our analysis of the superconducting order parameter by the means of temperature-dependent magnetic penetration depth λ (T) reveals a fully gapped superconducting state that can be well-fitted using an s -wave symmetric gap. We find that PdTe 2 is a promising model system for the investigation and interplay of nontrivial topology, surface superconductivity, and type-II bulk superconductivity in a van der

	Waals material. Moreover, our results indicate that the superconductivity in this material can be easily modified from type-I to type-II by disorder in the system.
83.	Unveiling the antibacterial and antifungal potential of biosynthesized silver nanoparticles from Chromolaena odorata leaves AK Bishoyi, CR Sahoo, P Samal, **NP Mishra**… - Scientific reports, 2024 **Abstract:** This research investigates the biogenic synthesis of silver nanoparticles (AgNPs) using the leaf extract of Chromolaena odorata (Asteraceae) and their potential as antibacterial and antifungal agents. Characterization techniques like ultraviolet-visible, Fourier transform infrared (FTIR), Dynamic light scattering and zeta potential (DLS), X-ray diffraction (XRD), transmission electron microscopy (TEM), and field emission scanning electron microscopy and energy-dispersive X-ray spectroscopy (FESEM-EDX) confirmed the formation of spherical (AgNPs). UV-vis spectroscopy reaffirms AgNP formation with a peak at 429 nm. DLS and zeta potential measurements revealed an average size of 30.77 nm and a negative surface charge (-0.532 mV). Further, XRD analysis established the crystalline structure of the AgNPs. Moreover, the TEM descriptions indicate that the AgNPs are spherical shapes, and their sizes ranged from 9 to 22 nm with an average length of 15.27 nm. The X-ray photoelectron spectroscopy (XPS) analysis validated the formation of metallic silver and elucidated the surface state composition of AgNPs. Biologically, CO-AgNPs showed moderate antibacterial activity but excellent antifungal activity against Candida tropicalis (MCC 1559) and Trichophyton rubrum (MCC 1598). Low MIC values (0.195 and 0.390 mg/mL) respectively, suggest their potential as effective antifungal agents. This suggests potential applications in controlling fungal infections, which are often more challenging to treat than bacterial infections. Molecular docking results validated that bioactive compounds in C. odorata contribute to antifungal activity by interacting with its specific domain. Further research could pave the way for the development of novel and safe antifungal therapies based on biogenic nanoparticles.
84.	Vertically aligned MoS2/ZnO heterostructure for highly selective NH3 sensing at room temperature **R Gond, P Shukla,** B Prakash, **B Rawat** - ACS Applied Electronic Materials, 2024 **Abstract:** The proliferation of the Internet of Things and Artificial Intelligence has fueled the demand for gas sensors operating at room temperature (RT), which can enable the development of ultralow power consumption devices for large-scale networking. Molybdenum disulfide (MoS2) shows great promise as a sensing layer material for near-RT chemiresistive sensors due to its larger specific surface area and high chemical-sensing capabilities over conventional metal oxide-based sensing materials. However, the horizontally aligned MoS2-based sensors have presented several challenges, such as poor response, low sensitivity, and incomplete recovery, for near-RT gas sensing. To address these limitations, we develop vertically aligned (VA) MoS2/ZnO heterostructure sensors for highly sensitive and selective detection of NH3 analyte. The fabricated VA-MoS2/ZnO heterostructure exhibits a high sensitivity value of 2.07%/ppm, excellent reproducibility, and stability with complete recovery at RT. Furthermore, the sensing performance of the heterostructure is investigated under the influence of temperature, humidity, and various ZnO concentrations. The sensor's superior performance is attributed to the enhancement in redox power of active sites in the vicinity of a 2D/0D heterointerface. This work offers a promising route to modulating the sensing behavior of VA-MoS2 that might be further exploited to expand its sensing capabilities. 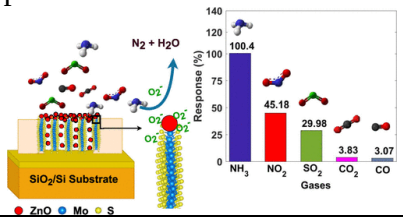

85.	Water wave interaction with ice-sheet of variable geometry in the presence of uniform current **A Aggarwal**, KK Barman, **SC Martha…** - Physics of Fluids, 2024 **Abstract:** We propose an asymptotic method to solve the problem of flexural-gravity wave scattering by an ice sheet of variable geometry in the presence of uniform currents. The significance of the article resides in the development of first and second-order solutions via the use of asymptotic expansion and the Fourier transform technique. We consider two different shape functions for the plate geometry, namely, Gaussian and Gaussian oscillatory. For both shape functions, the first and second-order solutions result in a major impact of depth Froude numbers in hydrodynamic coefficients, emphasizing the crucial function of the higher-order solutions in understanding the current responsiveness. We also observe the occurrence of Bragg resonance for the Gaussian oscillatory shape. The depth Froude number alters the frequency of wave components that are most reflected, and wave action conservation causes a rise in the energy of reflected waves. The depth Froude numbers can induce a unique minimum in reflection coefficient, which is close to 0. An examination of plate deflection reveals that the elevation amplitude is substantially higher near the point where there is a peak of elastic plate's shape. The pressure exerted by the plate is also concentrated near this point, highlighting the significance of the elastic plate's shape. The collective numerical observations for both shapes provide insight into resonance phenomena, the role of plate shape, and the intricate relationship between wave characteristics and varying plate properties. The findings from this study could assist geologists and marine engineers in designing and managing ice sheets, ports, and harbor infrastructure.

Disclaimer: This publication digest may not contain all the papers published. Library has compiled the publication data as per the alerts received from Scopus and Google Scholar for the affiliation “Indian Institute of Technology Ropar” for the month of April, 2024. The author(s) are requested to share their missing paper(s) details if any, for the inclusion in the next publication digest.